

THE SYMMETRIC GENERALIZED EIGENVALUE PROBLEM AS A NASH EQUILIBRIUM

Ian Gemp*

DeepMind

London, UK

imgemp@deepmind.com

Charlie Chen*

DeepMind

London, UK

ccharlie@deepmind.com

Brian McWilliams†

Google Research

Zürich, Switzerland

bmcw@google.com

ABSTRACT

The symmetric generalized eigenvalue problem (SGEP) is a fundamental concept in numerical linear algebra. It captures the solution of many classical machine learning problems such as canonical correlation analysis, independent components analysis, partial least squares, linear discriminant analysis, principal components and others. Despite this, most general solvers are prohibitively expensive when dealing with *streaming data sets* (i.e., minibatches) and research has instead concentrated on finding efficient solutions to specific problem instances. In this work, we develop a game-theoretic formulation of the top- k SGEP whose Nash equilibrium is the set of generalized eigenvectors. We also present a parallelizable algorithm with guaranteed asymptotic convergence to the Nash. Current state-of-the-art methods require $\mathcal{O}(d^2k)$ runtime complexity per iteration which is prohibitively expensive when the number of dimensions (d) is large. We show how to modify this parallel approach to achieve $\mathcal{O}(dk)$ runtime complexity. Empirically we demonstrate that this resulting algorithm is able to solve a variety of SGEP problem instances including a large-scale analysis of neural network activations.

1 INTRODUCTION

This work considers the symmetric generalized eigenvalue problem (SGEP),

$$Av = \lambda Bv \tag{1}$$

where A is symmetric and B is symmetric, positive definite. While the SGEP is not a common sight in modern machine learning literature, remarkably, it underlies several fundamental problems. Most obviously, when $A = X^\top X$, $B = I$, and X is a data matrix, we recover the ubiquitous SVD/PCA. However, by considering other forms of A and B we recover other well known problems. In general, we assume A and B consist of sums or expectations over outerproducts (e.g., $X^\top Y$ or $\mathbb{E}[xy^\top]$) to enable efficient matrix-vector products. These include, but are not limited to:

Canonical Correlation Analysis (CCA): Given a dataset of *paired* observations (or views) $x \in \mathbb{R}^{d_x}$ and $y \in \mathbb{R}^{d_y}$ (e.g., gene expressions x and medical imaging y corresponding to the same patient), CCA returns the linear projections of x and y that are maximally correlated. CCA is particularly useful for learning multi-modal representations of data and in semi-supervised learning (McWilliams et al., 2013); it is effectively the multi-view generalization of PCA (Guo & Wu, 2019) where A and B contain the cross- and auto-covariances of the two views respectively:

$$A = \begin{bmatrix} \mathbf{0} & \mathbb{E}[xy^\top] \\ \mathbb{E}[yx^\top] & \mathbf{0} \end{bmatrix} \quad B = \begin{bmatrix} \mathbb{E}[xx^\top] & \mathbf{0} \\ \mathbf{0} & \mathbb{E}[yy^\top] \end{bmatrix}. \tag{2}$$

*Asterisk denotes equal contribution.

†Work done while at DeepMind.

Independent Component Analysis (ICA): ICA seeks the directions in the data which are most structured, or alternatively, appear least Gaussian (Hyvärinen & Oja, 2000). A common SGEP formulation of ICA uncovers latent variables which maximize the non-Gaussianity of the data as defined by its excess kurtosis. ICA has famously been proposed as a solution to the so-called cocktail party source-separation problem in audio processing and has been used for denoising and more generally, the discovery of explanatory latent factors in data. Here A and B are the excess kurtosis and the covariance of the data respectively (Parra & Sajda, 2003):

$$A = \mathbb{E}[\langle x, x \rangle x x^\top] - \text{tr}(B)B - 2B^2 \quad B = \mathbb{E}[x x^\top]. \quad (3)$$

Normalized Graph Laplacians: The graph Laplacian matrix (L) is central to tasks such as spectral clustering ($A = L$, $B = I$) where its eigenvectors are known to solve a relaxation of min-cut (Von Luxburg, 2007). Alternatives, such as the random walk normalized Laplacian ($A = L$, B is the diagonal node-degree matrix), approximate other min-cut objectives. These normalized variants, in particular, are important to computing representations for learning value functions in reinforcement learning such as successor features (Machado et al., 2017a; Stachenfeld et al., 2014; Machado et al., 2017b), an extension of proto-value functions (Mahadevan, 2005) which uses the un-normalized graph Laplacian ($A = L$, $B = I$).

Partial least squares (PLS) can be formulated similarly to CCA and finds extensive use in chemometrics (Boucher et al., 2015), medical domains (Altmann et al., 2021) and beyond (McWilliams & Montana, 2010). Likewise, linear discriminant analysis (LDA) can be formulated as a SGEP and learns a label-aware projection of the data that separates classes well (Rao, 1948). More examples and uses of the SGEP can be found in (Bie et al., 2005; Borga et al., 1997). We now shift focus to the mathematical properties and challenges of the corresponding SGEP.

In this work, we assume the matrices A and B above can either be defined using expectations under a data distribution (e.g., $\mathbb{E}_{x \sim p(x)}[x x^\top]$) or means over a finite sample dataset (e.g., $\frac{1}{n} X^\top X$ where $X \in \mathbb{R}^{n \times d_x}$). In either case, we typically assume the data has mean zero unless specified otherwise.

Note that the SGEP, $Av = \lambda Bv$, is similar to the eigenvalue problem $B^{-1}Av = \lambda v$. There are two reasons for working with the SGEP instead: 1) inverting B is prohibitively expensive for a large matrix and 2) while A and $B \succ 0$ are symmetric, $B^{-1}A$ is not, which hides useful information about the eigenvalues and eigenvectors (they are necessarily real and B -orthogonal). This also highlights that the SGEP is a fundamentally more challenging problem than SVD and why a direct application of previous game-theoretic approaches such as (Gemp et al., 2021; 2022) is not possible.

The complexity of solving the SGEP is $\mathcal{O}(d^3)$ where d is the dimension of the square matrix A (equiv. B). Several libraries exist for solving the SGEP in-memory (Tzounas et al., 2020). There is also a vast numerics literature we cannot do justice that considers large matrices (Sorensen, 2002).

We specifically focus on the stochastic, streaming data setting which is of particular interest to machine learning methods which learn by iterating over small minibatches of data (e.g., stochastic gradient descent). Under this setting, machine learning research has developed simple approximate solvers for singular value decomposition (SVD) that scale to very large datasets (Allen-Zhu & Li, 2017b). Similarly, in this work, we contribute a simple, elegant solution to the SGEP, including

- A game whose Nash equilibrium is the top- k SGEP solution,
- An easily parallelizable algorithm with $\mathcal{O}(dk)$ per-iteration complexity relying only on matrix-vector products,
- An empirical analysis of neural similarity on activations $1000\times$ larger than prior work.

The game and accompanying algorithm are developed synergistically to achieve a formulation that is amenable to analysis and naturally leads to an elegant and efficient algorithm.

2 GENERALIZED EIGENGAME: PLAYERS, STRATEGIES, AND UTILITIES

In this work, we take the approach of defining the top- k SGEP as a k -player game. It is an open question how to define a k -player game appropriately such that key properties of the SGEP are

captured¹. As argued in previous work (Gemp et al., 2021; 2022), game formulations make obvious how computation can be distributed over players, leading to high parallelization, which is critical for processing large datasets. They have also clarified geometrical properties of the problem.

Specifically, we are interested in solving the top- k SGEP which means we are interested in finding the (unit-norm) generalized eigenvectors v_i associated with the top- k largest generalized eigenvalues λ_i . Therefore, let there be k **players** denoted $i \in \{1, \dots, k\}$, and let each select a vector \hat{v}_i (**strategy**) from the unit-sphere \mathcal{S}^{d-1} (*strategy space*). We define player i 's **utility** function conditioned on its parents (players $j < i$) as follows:

$$u_i(\hat{v}_i | \hat{v}_{j < i}) = \frac{\overbrace{\langle \hat{v}_i, A\hat{v}_i \rangle}^{\text{generalized Rayleigh Quotient}}}{\langle \hat{v}_i, B\hat{v}_i \rangle} - \sum_{j < i} \frac{\langle \hat{v}_j, A\hat{v}_j \rangle \langle \hat{v}_i, B\hat{v}_j \rangle^2}{\langle \hat{v}_j, B\hat{v}_j \rangle^2 \langle \hat{v}_i, B\hat{v}_i \rangle} \quad (4)$$

$$= \underbrace{\hat{\lambda}_i}_{\text{reward}} - \sum_{j < i} \underbrace{\hat{\lambda}_j \langle \hat{y}_i, B\hat{y}_j \rangle^2}_{\text{penalty}} \quad \text{where } \hat{y}_i = \frac{\hat{v}_i}{\|\hat{v}_i\|_B}, \quad (5)$$

$$\hat{\lambda}_i = \frac{\langle \hat{v}_i, A\hat{v}_i \rangle}{\langle \hat{v}_i, B\hat{v}_i \rangle}, \text{ and } \|z\|_B = \sqrt{\langle z, Bz \rangle}.$$

Player i 's utility has an intuitive explanation. The first term is recognized as the generalized Rayleigh quotient which can be derived by left multiplying both sides of the SGEP ($v^\top Av = \lambda v^\top Bv$) and solving for λ . Note that the generalized eigenvectors are guaranteed to be B -orthogonal, i.e., $v_i^\top Bv_j = 0$ for all $i \neq j$ (Appx. A Lemma 3). Therefore, the *reward* term incentivizes players to find directions that result in large eigenvalues, but are simultaneously *penalized* for choosing directions that align with their parents (players with index less than i , higher in the hierarchy). Finally, the penalty coefficient $\hat{\lambda}_j$ serves to balance the magnitude of the penalty terms with the reward term such that players have no incentive to ‘‘overlap’’ with parents. In Appx. B Proposition 4, we derive these same utilities via a *deflation* perspective. Next, we formally prove these utilities are well-posed in the sense that, given exact parents, their optima coincide with the top- k SGEP solution.

Lemma 1 (Well-posed Utilities). *Given exact parents and assuming the top- k eigenvalues of $B^{-1}A$ are distinct and positive, the maximizer of player i 's utility is the unique generalized eigenvector v_i (up to sign, i.e., $-v_i$ is also valid).*

Note that $\hat{\lambda}_i = \frac{\langle \hat{v}_i, A\hat{v}_i \rangle}{\langle \hat{v}_i, B\hat{v}_i \rangle} = \frac{\langle \hat{v}_i / \|\hat{v}_i\|_B, A\hat{v}_i / \|\hat{v}_i\|_B \rangle}{\langle \hat{v}_i / \|\hat{v}_i\|_B, B\hat{v}_i / \|\hat{v}_i\|_B \rangle} = \frac{\langle \hat{y}_i, A\hat{y}_i \rangle}{\langle \hat{y}_i, B\hat{y}_i \rangle}$, therefore, the results above still hold for utilities defined using vectors constrained to the unit ellipsoid, $\|\hat{y}_i\|_B = 1$, rather than the unit-sphere, $\|\hat{v}_i\|_I = 1$. However, in our setting, B is a massive matrix which can never be explicitly constructed and instead only observed via minibatches. It is then not clear how to handle the constraint $\|\hat{y}_i\|_B = 1$. We therefore only consider an approach that assumes $\|\hat{v}_i\|_I = 1$.

Next, we provide intuition for the shape of these utilities. Surprisingly, while non-concave, we prove analytically in Appx. B that they have a simple sinusoidal shape. A numerical illustration is given in Figure 1 to help the reader visualize this property.

Proposition 1 (Utility Shape). *Each player's utility is periodic in the angular deviation (θ) along the sphere. Its shape is sinusoidal, but with its angular axis (θ) smoothly deformed as a function of B . Most importantly, every local maximum is a global maximum.*

Figure 1 illustrates a primary difficulty of solving the SGEP over SVD. Due to the extreme differences in curvature caused by the B matrix, the SGEP should benefit from optimizers employing adaptive per-dimension learning rates. To our knowledge, this 1-d visualization of the difficulty of the SGEP is novel and we exploit this insight in experiments.

Finally, we formally define our proposed game and prove its equilibrium constitutes the top- k SGEP solution. We use the Greek letter **gamma** to denote *generalized*, and we differentiate between the game and the algorithm with upper Γ and lower case γ respectively.

Definition 1 (Γ -EigenGame). *Let Γ -EigenGame be the game with players $i \in \{1, \dots, k\}$, their strategy spaces $\hat{v}_i \in \mathcal{S}^{d-1}$, and their utilities u_i as defined in equation (5).*

¹The Courant-Fischer min-max principle poses the i th generalized eigenvalue as the solution to a two-player, zero-sum game (Parlett, 1998)—see Appx. A.2 for further discussion.

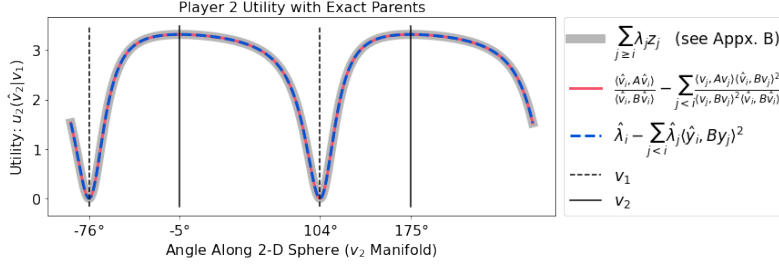


Figure 1: Each player’s utility is a sinusoid on the sphere warped tangentially along the axis of angular deviation according to B ; values for A and B used in this example are given in Appx. B. Three mathematical representations of the utility are plotted; their equivalence is supported by the overlapping curves. If player 2 aligns with the top eigenvector (dashed vertical), they receive zero utility. If they align with the second eigenvector (solid vertical), they receive λ_2 (optimal) as reward. If $B = I$ as in SVD/PCA, the vertical lines indicating the minima and maxima would be separated by exactly 90° . In this case, the matrix B redefines what it means for two vectors to be orthogonal ($\langle \hat{v}_i, B\hat{v}_j \rangle = 0$), so that the vectors are 71° (equivalently, $180^\circ - 71^\circ = 109^\circ$) from each other.

Theorem 1 (Nash Property). *Assuming the top- k generalized eigenvalues of the generalized eigenvalue problem $Av = \lambda Bv$ are positive and distinct, their corresponding generalized eigenvectors form the unique, strict Nash equilibrium of Γ -EigenGame.*

Proof. Lemma 1 proves that each generalized eigenvector v_i ($i \in \{1, \dots, k\}$) is the unique best response to v_{-i} , which implies the entire set constitutes the unique Nash equilibrium. \square

3 ALGORITHM: UNBIASED PLAYER UPDATES AND AUXILIARY VARIABLES

Given that Γ -EigenGame suitably captures the top- k SGEP, we now develop an iterative algorithm to approximate its solution. The basic approach we take is to perform parallel gradient ascent on all player utilities simultaneously. We focus on this approach in particular because it aligns with the predominant machine learning paradigm and hardware. We will first write down the gradient of each player’s utility and then introduce several simplifications for the purpose of enabling unbiased estimates in the stochastic setting.

Up to scaling factors, the gradient of player i ’s utility function with respect to \hat{v}_i is

$$\frac{(\hat{v}_i^\top B\hat{v}_i)A\hat{v}_i - (\hat{v}_i^\top A\hat{v}_i)B\hat{v}_i}{\langle \hat{v}_i, B\hat{v}_i \rangle^2} - \sum_{j < i} \frac{\hat{\lambda}_j}{\langle \hat{v}_j, B\hat{v}_j \rangle} (\hat{v}_i^\top B\hat{v}_j) \frac{[\langle \hat{v}_i, B\hat{v}_i \rangle B\hat{v}_j - \langle \hat{v}_i, B\hat{v}_j \rangle B\hat{v}_i]}{\langle \hat{v}_i, B\hat{v}_i \rangle^2}. \quad (6)$$

See Lemma 5 in Appx. B for a derivation of the gradient. Recall that B is a matrix that we intend to estimate with samples, i.e., it is a random variable, and it appears several times in the denominator of the gradient. Obtaining unbiased estimates of inverses of random variables is difficult (e.g., the naive approach gives an overestimate; $\mathbb{E}[1/x] \geq 1/\mathbb{E}[x]$ by Jensen’s inequality). We can remove the scalar $\langle \hat{v}_i, B\hat{v}_i \rangle^2$ in the denominator because it is common to all terms and will not change the direction of the gradient nor the location of fixed points; this step is critical to the design of our stochastic algorithm which we will explain later. We also use the following two additional relations:

- (i) $\hat{\lambda}_j \langle \hat{v}_i, B\hat{v}_j \rangle = \langle \hat{v}_i, A\hat{v}_j \rangle$ if player i ’s parents match their true solutions, i.e., $\hat{v}_{j < i} = v_{j < i}$,
- (ii) $\sqrt{\langle \hat{v}_j, B\hat{v}_j \rangle} = \|\hat{v}_j\|_B$ is strictly positive and real-valued because $B \succ 0$,

to arrive at the simplified update direction

$$\tilde{\nabla}_i = \overbrace{(\hat{v}_i^\top B\hat{v}_i)A\hat{v}_i - (\hat{v}_i^\top A\hat{v}_i)B\hat{v}_i}^{\text{reward}} - \sum_{j < i} \overbrace{(\hat{v}_i^\top A\hat{v}_j) [\langle \hat{v}_i, B\hat{v}_i \rangle B\hat{v}_j - \langle \hat{v}_i, B\hat{v}_j \rangle B\hat{v}_i]}^{\text{penalty}}. \quad (7)$$

Algorithm 1 Deterministic / Full-batch γ -EigenGame

```

1: Given:  $A \in \mathbb{R}^{d \times d}$  and  $B \in \mathbb{R}^{d \times d}$ , step size sequence  $\eta_t$ , and number of iterations  $T$ .
2:  $\hat{v}_i \sim \mathcal{S}^{d-1}$ , i.e.,  $\hat{v}_i \sim \mathcal{N}(\mathbf{0}_d, \mathbf{I}_d)$ ;  $\hat{v}_i \leftarrow \hat{v}_i / \|\hat{v}_i\|$  for all  $i$ 
3: for  $t = 1 : T$  do
4:   parfor  $i = 1 : k$  do
5:      $\hat{y}_j = \frac{\hat{v}_j}{\sqrt{\langle \hat{v}_j, B \hat{v}_j \rangle}}$ 
6:     rewards  $\leftarrow (\hat{v}_i^\top B \hat{v}_i) A \hat{v}_i - (\hat{v}_i^\top A \hat{v}_i) B \hat{v}_i$ 
7:     penalties  $\leftarrow \sum_{j < i} (\hat{v}_i^\top A \hat{y}_j) [\langle \hat{v}_i, B \hat{v}_i \rangle B \hat{y}_j - \langle \hat{v}_i, B \hat{y}_j \rangle B \hat{v}_i]$ 
8:      $\tilde{\nabla}_i \leftarrow \text{rewards} - \text{penalties}$ 
9:      $\hat{v}'_i \leftarrow \hat{v}_i + \eta_t \tilde{\nabla}_i$ 
10:     $\hat{v}_i \leftarrow \frac{\hat{v}'_i}{\|\hat{v}'_i\|}$ 
11:   end parfor
12: end for
13: return all  $\hat{v}_i$ 

```

Simplifying the gradient using (i) is sound because the hierarchy of players ensures the parents will be learned exactly asymptotically. For instance, player 1’s update has no penalty terms and so will converge asymptotically. The argument then proceeds by induction.

Note that B still appears in the denominator via the \hat{y}_j terms (recall equation (5)). We will revisit this issue later, but for now we will show this update converges to the desired solution given exact estimates of expectations (full-batch setting). Lemma 2 is a stepping stone to proving convergence with arbitrary parents in Theorem 2.

Lemma 2. *The direction $\tilde{\nabla}_i$ defined in equation (7) is a steepest ascent direction on utility $u_i(\hat{v}_i | \hat{v}_{j < i})$ given exact parents $\hat{v}_{j < i} = v_{j < i}$.*

Proof. This fact follows from the above argument that removing a positive scalar multiplier does not change the direction of the gradient of u_i w.r.t. \hat{v}_i and applying relation (i). \square

We present the deterministic version of γ -EigenGame in Algorithm 1 where k players use $\tilde{\nabla}_i$ in (7) to maximize their utilities in parallel (see **parfor**-loop below). While simultaneous gradient ascent fails to converge to Nash equilibria in games in general, it succeeds in this case because the hierarchy we impose ensures each player has a unique best response (Lemma 1); this type of procedure is known as *iterative strict dominance* in the game theory literature. Theorem 2, proven in Appx. E, guarantees it converges asymptotically to the true solution.

Theorem 2 (Deterministic / Full-batch Global Convergence). *Given a symmetric matrix A and symmetric positive definite matrix B where the top- k eigengaps of $B^{-1}A$ are positive along with a square-summable, not summable step size sequence η_t (e.g., $1/t$), Algorithm 1 converges to the top- k generalized eigenvectors asymptotically ($\lim_{T \rightarrow \infty}$) with probability 1.*

In the big data setting, A and B are statistical estimates, i.e., expectations of quantities over large datasets. Precomputing exact estimates is computationally expensive, so we assume a data model that allows drawing small *minibatches* of data at a time. Under such a model, stochastic approximation theory typically guarantees that as long as the update directions are *unbiased*, i.e., equal in expectation to the updates with exact estimates, then an appropriate algorithm will converge to the true solution.

In order to construct an unbiased update direction given access to minibatches of data, we need to draw multiple minibatches independently at random. We can construct an unbiased estimate of products of expectations, e.g., $(\hat{v}_i^\top B \hat{v}_i) A \hat{v}_i$, by drawing an independent batch for each, e.g., one for B and one for A . However, the B that appears in the denominator of \hat{y}_j is problematic; we cannot construct an unbiased estimate of the inverse of a random variable.

These problematic \hat{y}_j terms only appear in the penalties, which are a function of the parents’ eigenvector approximations. The first eigenvector has no parents, and so we can easily construct an unbiased estimate for it using multiple minibatches. We can then construct an unbiased estimate for

Algorithm 2 Stochastic γ -EigenGame

```

1: Given: paired data streams  $X_t \in \mathbb{R}^{b \times d_x}$  and  $Y_t \in \mathbb{R}^{b \times d_y}$ , number of parallel machines  $M$ 
   per player (minibatch size per machine  $b' = \frac{b}{M}$ ), step size sequences  $\eta_t$  and  $\gamma_t$ , scalar  $\rho$  lower
   bounding  $\sigma_{\min}(B)$ , and number of iterations  $T$ .
2:  $\hat{v}_i \sim \mathcal{S}^{d-1}$ , i.e.,  $\hat{v}_i \sim \mathcal{N}(\mathbf{0}_d, \mathbf{I}_d)$ ;  $\hat{v}_i \leftarrow \hat{v}_i / \|\hat{v}_i\|$  for all  $i$ 
3:  $[B\hat{v}]_i \leftarrow \hat{v}_i^0$  for all  $i$ 
4: for  $t = 1 : T$  do
5:   parfor  $i = 1 : k$  do
6:     parfor  $m = 1 : M$  do
7:       Construct  $A_{tm}$  and  $B_{tm}$  (*unbiased estimates using independent data batches)
8:        $\hat{y}_j = \frac{\hat{v}_j}{\sqrt{\max(\langle \hat{v}_j, [B\hat{v}]_j \rangle, \rho)}}$ 
9:        $[B\hat{y}]_j = \frac{[B\hat{v}]_j}{\sqrt{\max(\langle \hat{v}_j, [B\hat{v}]_j \rangle, \rho)}}$ 
10:      rewards  $\leftarrow (\hat{v}_i^\top B_{tm} \hat{v}_i) A_{tm} \hat{v}_i - (\hat{v}_i^\top A_{tm} \hat{v}_i) B_{tm} \hat{v}_i$ 
11:      penalties  $\leftarrow \sum_{j < i} (\hat{v}_i^\top A_{tm} \hat{y}_j) [\langle \hat{v}_i, B_{tm} \hat{v}_i \rangle [B\hat{y}]_j - \langle \hat{v}_i, [B\hat{y}]_j \rangle B_{tm} \hat{v}_i]$ 
12:       $\tilde{\nabla}_{im} \leftarrow \text{rewards} - \text{penalties}$ 
13:       $\nabla_{im}^{Bv} = (B_{tm} \hat{v}_i - [B\hat{v}]_i)$ 
14:    end parfor
15:     $\tilde{\nabla}_i \leftarrow \frac{1}{M} \sum_m [\tilde{\nabla}_{im}]$ 
16:     $\hat{v}'_i \leftarrow \hat{v}_i + \eta_t \tilde{\nabla}_i$ 
17:     $\hat{v}_i \leftarrow \frac{\hat{v}'_i}{\|\hat{v}'_i\|}$ 
18:     $\nabla_i^{Bv} \leftarrow \frac{1}{M} \sum_m [\nabla_{im}^{Bv}]$ 
19:     $[B\hat{v}]_i \leftarrow [B\hat{v}]_i + \gamma_t \nabla_i^{Bv}$ 
20:  end parfor
21: end for
22: return all  $\hat{v}_i$ 

```

each subsequent player by inductive reasoning. Intuitively, once the parents have been learned, \hat{v}_j should be stable and so it should be possible to estimate $B\hat{v}_j$ from a running average, and in turn, \hat{y}_j . This suggests introducing an auxiliary variable, denoted $[B\hat{v}]_j$ to track the running averages of $B\hat{v}_j$ (a similar approach is employed in (Pfau et al., 2018)). This effectively replaces $B\hat{y}_j$ with a non-random variable, avoiding the bias dilemma, at the expense of doubling the number of variables. Note that introducing this auxiliary variable implies the inner product $\langle \hat{v}_j, [B\hat{v}]_j \rangle$ may not be positive definite, therefore, we manually clip the result to be greater than or equal to ρ , the minimum singular value of B .

Precise pseudocode is given in Algorithm 2. Differences to Algorithm 1 are highlighted in color (auxiliary differences in blue, clipping in red). We point out that introducing an auxiliary variable for player i to track $[B\hat{v}]_i$ is not feasible because unlike player i 's parents' variables, \hat{v}_i cannot be assumed non-stationary. This is why removing $\langle \hat{v}_i, B\hat{v}_i \rangle^2$ earlier from the denominator of equation (6) was critical. Lastly, note that these modifications to the update are derived using an understanding of the intended computation and theoretical considerations; put shortly, *autograd* libraries will not uncover this solution. See Appx. E.2 for more discussion and analysis of Algorithm 2.

Computational Complexity and Parallelization. The naive, per-iteration runtime and work costs of this update are $\mathcal{O}(bdk^2)$ with batch size b , but due to the simplicity of the update (i.e., purely matrix-vector products), there are several opportunities for both model and data parallelism to reduce runtime cost to $\mathcal{O}(dk)$ (see Appx. I for steps). Note that low aggregate batch sizes can induce high gradient variance, slowing convergence (Durmus et al., 2021), making data parallelism desirable.

To give a concrete example, if each player (model) parallelizes over $M = b$ machines (data) as indicated by the two **parfor**-loops, the complexity reduces to $\mathcal{O}(dk)$. This is easy to implement with modern libraries, e.g., `pmap` using Jax, and as in prior work (Gemp et al., 2021), the communication of parents $v_{j < i}$ between machines is efficient in systems with fast interconnects (e.g., TPUs) although this presents a bottleneck we hope to alleviate in future work. Alternative parallel implementations are discussed in Appx. F. Lastly, the update consists purely of inexpensive

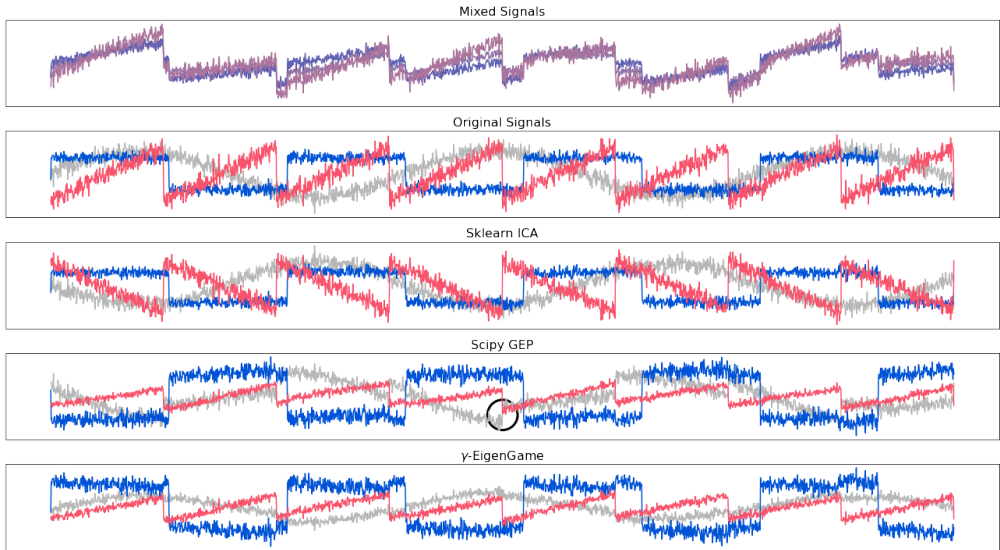


Figure 2: Blind Source Separation. Algorithm 2 (γ -EigenGame) run for 1000 epochs with mini-batches of size $\frac{n}{4}$ subsampled i.i.d. from the dataset recovers the three original signals from the linearly mixed signals. Scikit-learn’s FastICA² also recovers the signals by maximizing an alternative measure of non-Gaussianity. Directly solving the SGEP using `scipy.linalg.eigh(A, B)` fails to cleanly recover the gray sinusoid (black circle highlights a discontinuity) due to overfitting to the sample dataset. We confirm this by training γ -EigenGame for many more iterations and show it exhibits similar artifacts in Appx. G.

elementwise operations and matrix-vector products that can be computed quickly on deep learning hardware (e.g., GPUs and TPUs); unlike previous state-of-the-art in (Meng et al., 2021), no calls to CPU-bound linear algebra subroutines are necessary.

4 RELATED WORK

The SGEP is a fundamental problem in numerical linear algebra with numerous applications in machine learning and statistics. There is a long history in numerical computing of solving large SGEP problems (Sorensen, 2002; Knyazev & Skorokhodov, 1994; Golub & Ye, 2002; Aliaga et al., 2012; Klinvex et al., 2013). Many methods iterate with what can be viewed as “gradient-like” updates (D’yakonov & Knyazev, 1982; D’yakonov & Knyazev, 1992), however, they are not immediately applicable in the stochastic, streaming data setting. To our knowledge, efficient approaches for the SGEP or specific sub-problems (e.g., CCA) scale at best $\mathcal{O}(d^2k)$ in the streaming data setting.

Ge et al. (2016) give an algorithm for top- k SGEP that makes repeated use of a linear system solver to approximate the subspace of the true generalized eigenvectors, but may return an arbitrary rotation of the solution. While their method is theoretically efficient, it requires precomputing A and B which prohibits its use in a streaming data setting. The sequential least squares CCA algorithm proposed by Wang et al. (2016) similarly requires access to the full dataset up front, however, in their case, it is to ensure the generalized eigenvectors are exactly unit-norm relative to the matrix B . Allen-Zhu & Li (2017a) develop a SGEP algorithm that is theoretically linear in the size of the input (nd) and k , however, they assume access to the entire dataset (non-streaming). LOBPCG (Knyazev, 2017) is a non-streaming, Rayleigh maximizing technique with line-search and a preconditioned gradient.

Arora et al. (2017) propose a convex relaxation of the CCA problem along with a streaming algorithm with convergence guarantees. However, instead of learning $V_x \in \mathbb{R}^{d_x}$ and $V_y \in \mathbb{R}^{d_y}$ directly, it learns $M = V_x V_y^T \in \mathbb{R}^{d_x \times d_y}$ which is prohibitively expensive to store in memory for high-dimensional problems. Moreover, the complexity of this algorithm is $\mathcal{O}(d^3)$ due to an expensive projection step requiring an SVD of M . They propose an alternative version *without* guarantees that reduces the cost per iteration to $\mathcal{O}(dk^2)$.

²Run with `logcosh` approximation to negentropy (see (Hyvärinen & Oja, 2000) for explanation).

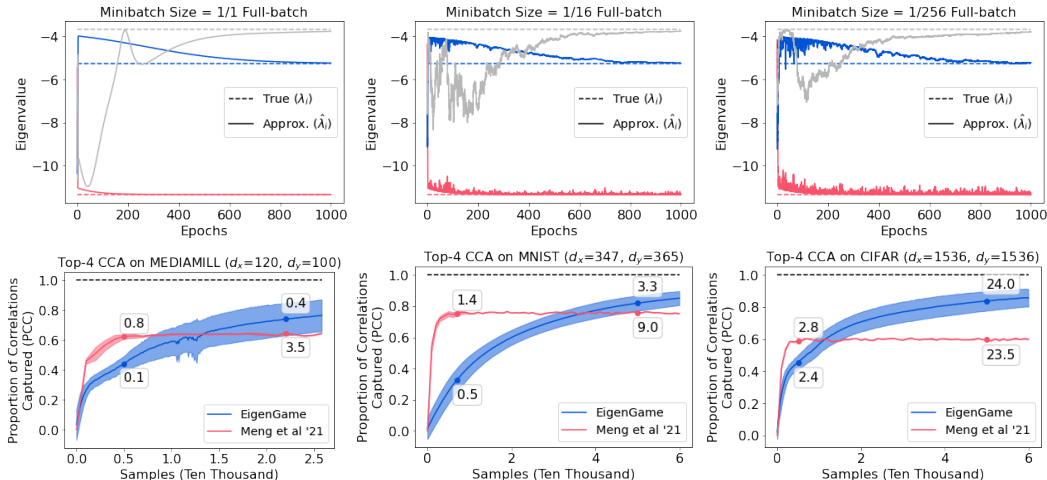


Figure 3: **Top:** γ -EigenGame converges to the true SGEP solution regardless of minibatch size in support of the unbiased nature of the derived update scheme (Algorithm 2). See Appx. G.2 for additional experiments showing learning in sequence performs worse than its parallel counterpart above. **Bottom:** γ -EigenGame compared to (Meng et al., 2021) on *proportion of correlations captured*— $\sum_i^k \hat{\lambda}_i / \sum_i^k \lambda_i$. Shading indicates ± 1 stdev. Markers indicate runtime in seconds.

Gao et al. (2019) also consider the streaming setting, but instead focus on top-1 CCA and like (Wang et al., 2016) and (Allen-Zhu & Li, 2017a), use shift-invert preconditioning to accelerate convergence. Bhatia et al. (2018) solves top-1 SGEP in the streaming setting.

Most recently, Meng et al. (2021) proposed a method to estimate top- k CCA in a streaming setting. Their algorithm requires several expensive Riemmanian optimization subroutines, giving a per iteration complexity of $\mathcal{O}(d^2k)$. Their convergence guarantee is in terms of subspace error, so as mentioned above, the projection matrices V_x and V_y may be rotations of their ordered (by correlation) counterparts. Their approach is the current state-of-the-art when considering CCA in the streaming setting for large datasets.

5 EXPERIMENTS

We demonstrate our proposed stochastic approach, Algorithm 2, on solving ICA and CCA via their SGEP formulations, and provide empirical support for its veracity. A Jax implementation is available at github.com/deepmind/eigengame. Scipy’s `linalg.eigh(A, B)` (Virtanen et al., 2020) is treated as ground truth when the data size permits. Hyperparameters are listed in Appx. H.

Independent Components Analysis. ICA can be used to disentangle mixed signals such as in the cocktail party problem. Here, we use the SGEP formulation to unmix three linearly mixed signals. Note that because the SGEP learns a linear unmixing of the data, the magnitude (and sign) of the original signals cannot be learned. Any change in the magnitude of a signal extracted by the SGEP can be offset by adjusting the magnitude and sign of a mixing weight.

We replicate a synthetic experiment from `scikit-learn` (Pedregosa et al., 2011) and compare Algorithm 2 to several approaches. Figure 2 shows our stochastic approach (γ -EigenGame) is able to recover the shapes of the original signals (length $n = 2000$ time series).

Implicit Regularization via Fixed Step Size Updates. Note that if we run Algorithm 2 for $100\times$ more iterations with $1/10$ th the step size, we converge to the exact SGEP solution (as found by `scipy`) and see similar artifacts in the extracted signals due to overfitting. Recently, Durmus et al. (2021) proved that fixed step size Riemannian approximation schemes converge to a stationary distribution around their solutions, which suggests γ -EigenGame enjoys a natural regularization property and explains its high performance on this the unmixing task. In Appx. G, we show that it is difficult to achieve similar results with `scipy` by regularizing A or B directly (e.g., $A + \epsilon I$) prior to calling `scipy.linalg.eigh`.

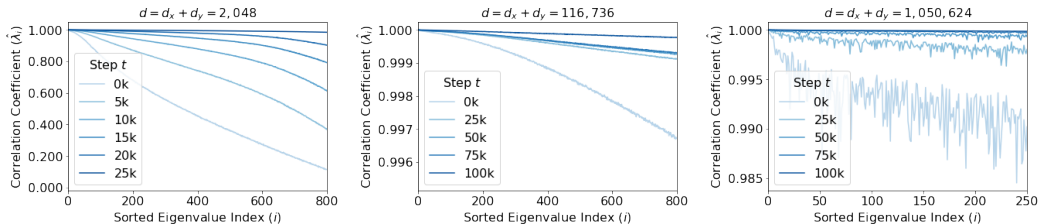


Figure 4: γ -EigenGame compares the representation (activations) of a deep network trained on CIFAR-10 for t steps to that of its final learned representation (25k or 100k steps). Curves with higher correlation coefficients indicate more similar representations.

Unbiased Updates. We empirically support our claim that the fixed point of Algorithm 2 is unbiased regardless of minibatch size.³ Not only does γ -EigenGame recover the same generalized eigenvalues, but the top row of figure 3 also suggests that the algorithm takes a similar trajectory for each minibatch size.

Canonical Correlations Analysis. Here, we use γ -EigenGame to linearly project multimodal datasets into lower-dimensional spaces such that they are maximally correlated. As discussed in related work, several approaches have been developed to extend CCA to streaming, high-dimensional datasets. Recall that our approach has per-iteration complexity $\mathcal{O}(bdk)$ with the previous state-of-the-art in the streaming setting having $\mathcal{O}(d^2k)$ (Meng et al., 2021). We replicate the experiments of (Meng et al., 2021) and compare against their approach on three datasets.

The bottom row of figure 3 shows our approach is competitive with (Meng et al., 2021). We also point out that while the previous approach by Meng et al. (2021) enjoys theoretical convergence guarantees with rates, it appears to slow in progress near a biased solution. These datasets are low dimensional ($d \leq 3072$), so we are able to obtain ground truth eigenvectors efficiently using `scipy`. Our next set of experiments considers much higher dimensional where a naive call to `scipy` fails.

Large-scale Neural Network Analysis. Recently, CCA has been used to aid in interpreting the representations of deep neural networks (Raghu et al., 2017; Morcos et al., 2018; Kornblith et al., 2019). These approaches are restricted to layer-wise comparisons of representations, reduced-dimensionality views of representations (via PCA), or small dataset sizes to accommodate current limits of CCA approaches. We replicate one of their analyses (specifically Fig. 1a of (Morcos et al., 2018)) on the activations of an entire network (not just a layer), unblocking this type of analysis for larger deep learning models.

The largest dimensions handled in (Raghu et al., 2017) are $\mathcal{O}(10^3)$. Figure 4 demonstrates our approach (parallelized over 8 TPU chips) on $\mathcal{O}(10^3)$ dimensions (left), $\mathcal{O}(10^5)$ dimensions (middle), and $\mathcal{O}(10^6)$ dimensions (right). Note that in these experiments, we are loading minibatches of CIFAR-10 images, running them through a deep convolutional network, harvesting the activations, and then passing them to our distributed γ -EigenGame solver. As mentioned in Section 2, our understanding of the geometry of the utilities suggests replacing the standard gradient ascent on \hat{v}_i with Adam (Kingma & Ba, 2014); Adam exhibits behavior that implicitly improves stability around equilibria (Gemp & McWilliams, 2019). For the smaller $\mathcal{O}(10^3)$ setting, where we can exactly compute ground truth using `scipy`, we confirm that our approach converges to the top-1024 (out of 2048 possible) eigenvectors with a subspace error of 0.002 (see Appx. A).

6 CONCLUSION

We presented Γ -EigenGame, a game-theoretic formulation of the generalized eigenvalue problem (SGEP). Our formulation enabled the development of a novel algorithm that scales to massive streaming datasets. The SGEP underlies many classical data processing tools across the sciences, and we believe our proposed approach unblocks its use on the ever-growing size of modern datasets in the streaming setting. In particular, it achieves this by parallelizing computation using modern AI-centric distributed compute infrastructure such as GPUs and TPUs.

³The gray line converges last because we chose to minimize rather than maximize kurtosis.

Acknowledgements. We thank Claire Vernade for reviewing the paper and proofs and early discussions. Thore Graepel for early discussions. Zhe Wang for guidance on engineering. Sukhdeep Singh for project management.

REFERENCES

- Jose I Aliaga, Paolo Bientinesi, Davor Davidović, Edoardo Di Napoli, Francisco D Igual, and Enrique S Quintana-Orti. Solving dense generalized eigenproblems on multi-threaded architectures. *Applied mathematics and computation*, 218(22):11279–11289, 2012.
- Zeyuan Allen-Zhu and Yuanzhi Li. Doubly accelerated methods for faster cca and generalized eigendecomposition. In *International Conference on Machine Learning*, pp. 98–106. PMLR, 2017a.
- Zeyuan Allen-Zhu and Yuanzhi Li. First efficient convergence for streaming k-PCA: a global, gap-free, and near-optimal rate. In *2017 IEEE 58th Annual Symposium on Foundations of Computer Science (FOCS)*, pp. 487–492. IEEE, 2017b.
- Andre Altmann, Neda Jahanshad, Paul M Thompson, and Marco Lorenzi. Partial least squares provides a whole-genome whole-brain imaging genetics approach. 2021.
- Raman Arora, Teodor Vanislavov Marinov, Poorya Mianjy, and Nati Srebro. Stochastic approximation for canonical correlation analysis. *Advances in Neural Information Processing Systems*, 30, 2017.
- Haim Avron. A generalized courant-fischer minimax theorem. 2008.
- Kush Bhatia, Aldo Pacchiano, Nicolas Flammarion, Peter L Bartlett, and Michael I Jordan. Genoja: Simple & efficient algorithm for streaming generalized eigenvector computation. *Advances in neural information processing systems*, 31, 2018.
- Tijl De Bie, Nello Cristianini, and Roman Rosipal. Eigenproblems in pattern recognition. In *Handbook of geometric computing*, pp. 129–167. Springer, 2005.
- Magnus Borga, Tomas Landelius, and Hans Knutsson. *A unified approach to PCA, PLS, MLR and CCA*. Linköping University, Department of Electrical Engineering, 1997.
- Thomas F Boucher, Marie V Ozanne, Marco L Carmosino, M Darby Dyar, Sridhar Mahadevan, Elly A Breves, Kate H Lepore, and Samuel M Clegg. A study of machine learning regression methods for major elemental analysis of rocks using laser-induced breakdown spectroscopy. *Spectrochimica Acta Part B: Atomic Spectroscopy*, 107:1–10, 2015.
- Li Deng. The mnist database of handwritten digit images for machine learning research. *IEEE Signal Processing Magazine*, 29(6):141–142, 2012.
- Alain Durmus, Pablo Jiménez, Éric Moulines, and SAID Salem. On riemannian stochastic approximation schemes with fixed step-size. In *International Conference on Artificial Intelligence and Statistics*, pp. 1018–1026. PMLR, 2021.
- EG D’yakonov and AV Knyazev. Group iterative method for finding lower-order eigenvalues. *Moscow University Computational Mathematics and Cybernetics*, 15:32–40, 1982.
- EG D’yakonov and AV Knyazev. On an iterative method for finding lower eigenvalues. *Russian Journal of Numerical Analysis and Mathematical Modeling*, 1992.
- Chao Gao, Dan Garber, Nathan Srebro, Jialei Wang, and Weiran Wang. Stochastic canonical correlation analysis. *J. Mach. Learn. Res.*, 20:167–1, 2019.
- Rong Ge, Chi Jin, Sham M. Kakade, Praneeth Netrapalli, and Aaron Sidford. Efficient algorithms for large-scale generalized eigenvector computation and canonical correlation analysis. In *International Conference on Machine Learning*, pp. 2741–2750. PMLR, 2016.
- Ian Gemp and Brian McWilliams. The unreasonable effectiveness of adam on cycles. In *NeurIPS Workshop on Bridging Game Theory and Deep Learning*, 2019.

- Ian Gemp, Brian McWilliams, Claire Vernade, and Thore Graepel. Eigengame: PCA as a Nash equilibrium. In *International Conference for Learning Representations*, 2021.
- Ian Gemp, Brian McWilliams, Claire Vernade, and Thore Graepel. Eigengame unloaded: When playing games is better than optimizing. *International Conference for Learning Representations*, 2022.
- Gene H Golub and Qiang Ye. An inverse free preconditioned krylov subspace method for symmetric generalized eigenvalue problems. *SIAM Journal on Scientific Computing*, 24(1):312–334, 2002.
- Navin Goyal and Abhishek Shetty. Sampling and optimization on convex sets in riemannian manifolds of non-negative curvature. In *Conference on Learning Theory*, pp. 1519–1561. PMLR, 2019.
- Chenfeng Guo and Dongrui Wu. Canonical correlation analysis (CCA) based multi-view learning: An overview. *arXiv preprint arXiv:1907.01693*, 2019.
- Charles R. Harris, K. Jarrod Millman, Stéfan J. van der Walt, Ralf Gommers, Pauli Virtanen, David Cournapeau, Eric Wieser, Julian Taylor, Sebastian Berg, Nathaniel J. Smith, Robert Kern, Matti Picus, Stephan Hoyer, Marten H. van Kerkwijk, Matthew Brett, Allan Haldane, Jaime Fernández del Río, Mark Wiebe, Pearu Peterson, Pierre Gérard-Marchant, Kevin Sheppard, Tyler Reddy, Warren Weckesser, Hameer Abbasi, Christoph Gohlke, and Travis E. Oliphant. Array programming with NumPy. *Nature*, 585(7825):357–362, September 2020. doi: 10.1038/s41586-020-2649-2. URL <https://doi.org/10.1038/s41586-020-2649-2>.
- Aapo Hyvärinen and Erkki Oja. Independent component analysis: algorithms and applications. *Neural networks*, 13(4-5):411–430, 2000.
- Diederik P Kingma and Jimmy Ba. Adam: A method for stochastic optimization. *arXiv preprint arXiv:1412.6980*, 2014.
- A Klinvex, Faisal Saied, and A Sameh. Parallel implementations of the trace minimization scheme tracemin for the sparse symmetric eigenvalue problem. *Computers & Mathematics with Applications*, 65(3):460–468, 2013.
- Andrew Knyazev. Recent implementations, applications, and extensions of the locally optimal block preconditioned conjugate gradient method (LOBPCG). *arXiv preprint arXiv:1708.08354*, 2017.
- Andrew V Knyazev and Alexander L Skorokhodov. Preconditioned gradient-type iterative methods in a subspace for partial generalized symmetric eigenvalue problems. *SIAM journal on numerical analysis*, 31(4):1226–1239, 1994.
- Simon Kornblith, Mohammad Norouzi, Honglak Lee, and Geoffrey Hinton. Similarity of neural network representations revisited. In *International Conference on Machine Learning*, pp. 3519–3529. PMLR, 2019.
- Alex Krizhevsky, Geoffrey Hinton, et al. Learning multiple layers of features from tiny images. 2009.
- Yuanyuan Liu, Fanhua Shang, James Cheng, Hong Cheng, and Licheng Jiao. Accelerated first-order methods for geodesically convex optimization on Riemannian manifolds. In *Advances in Neural Information Processing Systems*, pp. 4868–4877, 2017.
- Marlos C Machado, Marc G Bellemare, and Michael Bowling. A laplacian framework for option discovery in reinforcement learning. In *International Conference on Machine Learning*, pp. 2295–2304. PMLR, 2017a.
- Marlos C Machado, Clemens Rosenbaum, Xiaoxiao Guo, Miao Liu, Gerald Tesauro, and Murray Campbell. Eigenoption discovery through the deep successor representation. *arXiv preprint arXiv:1710.11089*, 2017b.
- Sridhar Mahadevan. Proto-value functions: developmental reinforcement learning. In *Proceedings of the International Conference on Machine learning*, pp. 553–560, 2005.

- MATLAB. *9.7.0.1190202 (R2019b)*. The MathWorks Inc., Natick, Massachusetts, 2018.
- Brian McWilliams and Giovanni Montana. Sparse partial least squares regression for on-line variable selection with multivariate data streams. *Statistical Analysis and Data Mining: The ASA Data Science Journal*, 3(3):170–193, 2010.
- Brian McWilliams, David Balduzzi, and Joachim M Buhmann. Correlated random features for fast semi-supervised learning. In *Advances in Neural Information Processing Systems*, pp. 440–448, 2013.
- Zihang Meng, Rudrans Chakraborty, and Vikas Singh. An online riemannian pca for stochastic canonical correlation analysis. *Advances in Neural Information Processing Systems*, 34, 2021.
- Ari Morcos, Maithra Raghu, and Samy Bengio. Insights on representational similarity in neural networks with canonical correlation. *Advances in Neural Information Processing Systems*, 31, 2018.
- Beresford N Parlett. *The symmetric eigenvalue problem*. SIAM, 1998.
- Lucas Parra and Paul Sajda. Blind source separation via generalized eigenvalue decomposition. *The Journal of Machine Learning Research*, 4:1261–1269, 2003.
- F. Pedregosa, G. Varoquaux, A. Gramfort, V. Michel, B. Thirion, O. Grisel, M. Blondel, P. Prettenhofer, R. Weiss, V. Dubourg, J. Vanderplas, A. Passos, D. Cournapeau, M. Brucher, M. Perrot, and E. Duchesnay. Scikit-learn: Machine learning in Python. *Journal of Machine Learning Research*, 12:2825–2830, 2011.
- David Pfau, Stig Petersen, Ashish Agarwal, David GT Barrett, and Kimberly L Stachenfeld. Spectral inference networks: Unifying deep and spectral learning. In *International Conference on Learning Representations*, 2018.
- Maithra Raghu, Justin Gilmer, Jason Yosinski, and Jascha Sohl-Dickstein. SVCCA: Singular vector canonical correlation analysis for deep learning dynamics and interpretability. In *Advances in Neural Information Processing Systems*, pp. 6076–6085, 2017.
- C Radhakrishna Rao. The utilization of multiple measurements in problems of biological classification. *Journal of the Royal Statistical Society. Series B (Methodological)*, 10(2):159–203, 1948.
- Suhail M Shah. Stochastic approximation on Riemannian manifolds. *Applied Mathematics & Optimization*, pp. 1–29, 2019.
- Cees GM Snoek, Marcel Worring, Jan C Van Gemert, Jan-Mark Geusebroek, and Arnold WM Smeulders. The challenge problem for automated detection of 101 semantic concepts in multimedia. In *Proceedings of the 14th ACM international conference on Multimedia*, pp. 421–430, 2006.
- Danny C Sorensen. Numerical methods for large eigenvalue problems. *Acta Numerica*, 11:519–584, 2002.
- Kimberly L Stachenfeld, Matthew Botvinick, and Samuel J Gershman. Design principles of the hippocampal cognitive map. *Advances in neural information processing systems*, 27, 2014.
- Vincent Tan, Nick Firoozye, and Stefan Zohren. Canonical portfolios: Optimal asset and signal combination. *arXiv preprint arXiv:2202.10817*, 2022.
- Cheng Tang. Exponentially convergent stochastic k-PCA without variance reduction. In *Advances in Neural Information Processing Systems*, pp. 12393–12404, 2019.
- Georgios Tzounas, Ioannis Dassios, Muyang Liu, and Federico Milano. Comparison of numerical methods and open-source libraries for eigenvalue analysis of large-scale power systems. *Applied Sciences*, 10(21):7592, 2020.

Pauli Virtanen, Ralf Gommers, Travis E. Oliphant, Matt Haberland, Tyler Reddy, David Cournapeau, Evgeni Burovski, Pearu Peterson, Warren Weckesser, Jonathan Bright, Stéfan J. van der Walt, Matthew Brett, Joshua Wilson, K. Jarrod Millman, Nikolay Mayorov, Andrew R. J. Nelson, Eric Jones, Robert Kern, Eric Larson, C J Carey, İlhan Polat, Yu Feng, Eric W. Moore, Jake VanderPlas, Denis Laxalde, Josef Perktold, Robert Cimrman, Ian Henriksen, E. A. Quintero, Charles R. Harris, Anne M. Archibald, Antônio H. Ribeiro, Fabian Pedregosa, Paul van Mulbregt, and SciPy 1.0 Contributors. SciPy 1.0: Fundamental Algorithms for Scientific Computing in Python. *Nature Methods*, 17:261–272, 2020. doi: 10.1038/s41592-019-0686-2.

Ulrike Von Luxburg. A tutorial on spectral clustering. *Statistics and Computing*, 17(4):395–416, 2007.

Weiran Wang, Jialei Wang, Dan Garber, and Nati Srebro. Efficient globally convergent stochastic optimization for canonical correlation analysis. *Advances in Neural Information Processing Systems*, 29, 2016.

Appendix: The Symmetric Generalized Eigenvalue Problem as a Nash Equilibrium

A PRELIMINARIES: GENERALIZED EIGENVALUE PROBLEM

The following known properties of the SGEP are useful for our analysis and broadening the scope of SGEP applications.

Lemma 3 (*B-orthogonality*). $v_i^\top B v_j = v_j^\top B v_i = 0$ for any distinct pair of generalized eigenvectors of $Av = \lambda Bv$ where A is symmetric and B is symmetric positive definite.

Proof. Consider the eigenvalue problem $B^{-\frac{1}{2}}AB^{-\frac{1}{2}}w = \lambda w$. Let v be a generalized eigenvector of the generalized eigenvalue problem $Av = \lambda'Bv$. Then the former eigenvalue problem is solved by $w = B^{\frac{1}{2}}v$. By inspection, $B^{-\frac{1}{2}}AB^{-\frac{1}{2}}w = B^{-\frac{1}{2}}AB^{-\frac{1}{2}}B^{\frac{1}{2}}v = B^{-\frac{1}{2}}Av = \lambda'B^{-\frac{1}{2}}Bv = \lambda'B^{\frac{1}{2}}v = \lambda'w$. Direct computation of the Rayleigh quotients for both problems reveals $\lambda = \lambda'$. Note that B is positive definite, i.e., full-rank, establishing a bijection between v and w : $v = B^{-\frac{1}{2}}w$. Also, note that $B^{-\frac{1}{2}}AB^{-\frac{1}{2}}$ is symmetric because A and B are symmetric, therefore, w may be chosen such that $W^\top W = I$ which implies $w_i^\top w_j = \delta_{ij} = v_i^\top B^{\frac{1}{2}}B^{\frac{1}{2}}v_j = v_i^\top Bv_j$, i.e., the generalized eigenvectors are B -orthogonal. \square

Proposition 2 (*Similar Matrices*). Given symmetric matrices A and $B \succ 0$, consider the generalized eigenvalue problem $Av = \lambda'Bv$ with λ' and v its corresponding generalized eigenvalues and eigenvectors. Then the eigenvectors and eigenvalues of the related eigenvalue problem $B^{-\frac{1}{2}}AB^{-\frac{1}{2}}w = \lambda w$ are $w = B^{\frac{1}{2}}v$ and $\lambda = \lambda'$.

Proof. The relationship between the eigenvectors of the two problems is proven in Lemma 3. The relationship between the eigenvalues can be proven by inspection after calculating the Rayleigh quotients for both problems:

$$\lambda' = \frac{v^\top Av}{v^\top Bv} \quad (8)$$

$$\lambda = \frac{w^\top B^{-\frac{1}{2}}AB^{-\frac{1}{2}}w}{w^\top w} \quad (9)$$

$$= \frac{v^\top B^{\frac{1}{2}}B^{-\frac{1}{2}}AB^{-\frac{1}{2}}B^{\frac{1}{2}}v}{v^\top Bv} \quad (10)$$

$$= \frac{v^\top Av}{v^\top Bv} \quad (11)$$

$$= \lambda'. \quad (12)$$

\square

A.1 COMPUTING SUBSPACE ERROR FOR SGEP

Lemma 3 states that the generalized eigenvectors are B -orthogonal rather than orthogonal under the standard Euclidean basis. Therefore, we cannot compute subspace error in the same way as is typically done for e.g., singular value decomposition. However, we can exploit Lemma 2 to compute subspace error for the related eigenvalue problem $B^{-\frac{1}{2}}AB^{-\frac{1}{2}}w = \lambda w$ which *does* have orthogonal eigenvectors due to its symmetry.

Formally, let v be a solution to the SGEP, $Av = \lambda'Bv$. Then by Lemma 2, $w = B^{1/2}v$ is a solution to $B^{-1/2}AB^{-1/2}w = \lambda w$, with eigenvalue $\lambda = \lambda'$. Leveraging this equivalence, we can measure subspace error of the SGEP solution by first mapping it to the normalized case and computing subspace error there where W contains the top- k eigenvectors of $B^{-1/2}AB^{-1/2}$. Also let $\hat{W} = B^{1/2}\hat{V}$ where \hat{V} contains our top- k approximations. Given the top- k ground truth eigenvectors W

and approximations W , normalized subspace error can then be computed as $1 - \frac{1}{k} \text{tr}(U^* P) \in [0, 1]$ where $U^* = WW^\top$ and $P = \hat{W}\hat{W}^\top$ (Gemp et al., 2021; Tang, 2019).

A.2 COURANT-FISCHER MIN-MAX PRINCIPLE

The Courant-Fischer Min-Max principle states that the i th largest generalized eigenvalue is given by the *minimum* possible Rayleigh quotient within the i -dimensional subspace S that captures *maximal* trace (Avron, 2008; Parlett, 1998):

$$v_i = \arg \min_{v_i \in S} \max_{\dim(S)=i} \frac{v_i^\top A v_i}{v_i^\top B v_i}. \quad (13)$$

Note this defines each eigenvalue of the SGEP as the value (at Nash equilibrium) of a min-max (two-player, zero-sum) game rather than the entire set of top- k eigenvectors/eigenvalues as the Nash equilibrium / utility-at-Nash of a k -player, general-sum game.

B Γ -EIGENGAME IS WELL-POSED

First, we prove Γ -EigenGame suitably captures the top- k SGEP.

Lemma 1 (Well-posed Utilities). *Given exact parents and assuming the top- k eigenvalues of $B^{-1}A$ are distinct and positive, the maximizer of player i 's utility is the unique generalized eigenvector v_i (up to sign, i.e., $-v_i$ is also valid).*

Proof. Approach: We will represent each \hat{v}_i as a linear combination of the true eigenvectors, v_p for $p \in \{1, d\}$. We will then show that maximizing the utility for each player with exact parents is equivalent to solving a linear program. This resulting problem has a unique solution, which is the true eigenvector v_i .

Assume the parents have been learned exactly and let $\hat{v}_i = \sum_p w_p v_p$ with $\|\hat{v}_i\| = 1$ and where w_p are the weights of the linear combination. Expand and simplify the following expressions that appear in the utility definition with the knowledge that the generalized eigenvectors are guaranteed to be B -orthogonal, i.e., $v_i^\top B v_j = 0$ for all $i \neq j$ (see Lemma 3 in appendix):

$$\langle \hat{v}_i, B \hat{v}_i \rangle = \left(\sum_p w_p v_p \right)^\top B \left(\sum_l w_l v_l \right) = \sum_p \sum_l w_p w_l v_p^\top B v_l = \sum_p w_p^2 \langle v_p, B v_p \rangle \quad (14)$$

$$\langle \hat{v}_i, A \hat{v}_i \rangle = \left(\sum_p w_p v_p \right)^\top A \left(\sum_l w_l v_l \right) = \sum_p \sum_l \lambda_l w_p w_l v_p^\top B v_l = \sum_p \lambda_p w_p^2 \langle v_p, B v_p \rangle \quad (15)$$

$$\langle \hat{v}_i, B v_j \rangle = \left(\sum_p w_p v_p \right)^\top B v_j = w_j \langle v_j, B v_j \rangle \quad (16)$$

$$\langle \hat{v}_i, A v_j \rangle = \left(\sum_p w_p v_p \right)^\top A v_j = \lambda_j w_j \langle v_j, B v_j \rangle. \quad (17)$$

Plugging these in to the utility function, we find

$$u_i(\hat{v}_i|v_{j<i}) = \frac{\langle \hat{v}_i, A\hat{v}_i \rangle}{\langle \hat{v}_i, B\hat{v}_i \rangle} - \sum_{j<i} \frac{\langle v_j, Av_j \rangle \langle \hat{v}_i, Bv_j \rangle^2}{\langle v_j, Bv_j \rangle^2 \langle \hat{v}_i, B\hat{v}_i \rangle} \quad (18)$$

$$= \frac{\langle \hat{v}_i, A\hat{v}_i \rangle}{\langle \hat{v}_i, B\hat{v}_i \rangle} - \sum_{j<i} \frac{\lambda_j \langle \hat{v}_i, Bv_j \rangle^2}{\langle v_j, Bv_j \rangle \langle \hat{v}_i, B\hat{v}_i \rangle} \quad \langle v_j, Av_j \rangle \rightarrow \langle v_j, \lambda_j Bv_j \rangle \quad (19)$$

$$= \frac{\langle \hat{v}_i, A\hat{v}_i \rangle}{\langle \hat{v}_i, B\hat{v}_i \rangle} - \sum_{j<i} \frac{\langle \hat{v}_i, Av_j \rangle \langle \hat{v}_i, Bv_j \rangle}{\langle v_j, Bv_j \rangle \langle \hat{v}_i, B\hat{v}_i \rangle} \quad \langle \hat{v}_i, \lambda_j Bv_j \rangle \rightarrow \langle \hat{v}_i, Av_j \rangle \quad (20)$$

$$= \frac{1}{\sum_p w_p^2 \langle v_p, Bv_p \rangle} \left[\sum_l \lambda_l w_l^2 \langle v_l, Bv_l \rangle - \sum_{j<i} \frac{(\lambda_j w_j \langle v_j, Bv_j \rangle) (w_j \langle v_j, Bv_j \rangle)}{\langle v_j, Bv_j \rangle} \right] \quad (21)$$

$$= \sum_l \lambda_l z_l - \sum_{j<i} \lambda_j z_j = \sum_{j \geq i} \lambda_j z_j. \quad (22)$$

where

$$z_j = \frac{w_j^2 \langle v_j, Bv_j \rangle}{\sum_p w_p^2 \langle v_p, Bv_p \rangle} = \frac{w_j^2 b_j^2}{\sum_p w_p^2 b_p^2} = \frac{q_j^2}{\sum_p q_p^2} \quad (23)$$

and $z \in \Delta^{d-1}$.

This is a linear optimization problem over the simplex. Given that the eigenvalues are distinct and positive, we have that the unique solution is $z = e_i$, the onehot vector with a 1 at index i .

In order to prove uniqueness of w (up to sign), we apply Lemma 4, which proves a bijection (up to sign) between z and w , completing the proof. \square

Lemma 4. *Let $z \in \Delta^{d-1}$ such that $z_j = \frac{w_j^2 \langle v_j, Bv_j \rangle}{\sum_p w_p^2 \langle v_p, Bv_p \rangle}$ where w parameterizes the approximation $\hat{v}_i = \sum_p w_p v_p \in \mathcal{S}^{d-1}$. There exists a unique bijection (up to sign of w_j) between z_j and w_j , i.e., $w_j = \pm g(z)_j$.*

Proof. Let $b_j = \langle v_j, Bv_j \rangle$ and $q_j = w_j b_j$ so that $w_j = q_j/b_j$. Then $\hat{v}_i = \sum_p \frac{q_p}{b_p} v_p$. Also, $q_j^2 = cz_j$ where $c = \sum_p q_p^2$ so that q_j^2 is uniquely defined up to a scalar multiple, i.e., its direction is immediately unique by this formula but not its magnitude. Recall $\langle v_i, Bv_j \rangle = 0$ for all $i \neq j$ which implies $V^\top BV$ is diagonal. Therefore, the constraint $\|\hat{v}_i\| = \|w\|_{V^\top V}^2 = 1$ translates to $\| \frac{q}{b} \|_{V^\top V}^2 = q^\top (V^\top BV)^{-1/2} (V^\top V) (V^\top BV)^{-1/2} q = q^\top D^{-1} q = 1$. In other words, whereas an approximate eigenvector for the standard eigenvalue problem can be modeled as choosing a vector on the unit-sphere, an approximate eigenvector for the generalized eigenvalue problem is modeled as choosing a vector on an ellipsoid (D is positive definite because $V^\top V$ is symmetric positive definite assuming distinct eigenvalues, and we are given B is symmetric positive definite). This result uniquely defines a magnitude for q , therefore, combining it with the previous result uniquely defines w_j^2 from q_j^2 completing the bijection. The only degree of freedom that remains is the sign of w_j which is expected as both v_i and $-v_i$ are valid eigenvectors. \square

Although player i 's utility u_i appears abstruse, it actually has a simple explanation and structure.

Proposition 1 (Utility Shape). *Each player's utility is periodic in the angular deviation (θ) along the sphere. Its shape is sinusoidal, but with its angular axis (θ) smoothly deformed as a function of B . Most importantly, every local maximum is a global maximum (see Figure 1 for an example).*

Proof. Lemma 1 proves each utility function can be represented as a linear function over a simplex $z \in \Delta^{d-1}$. Lemma 4 then proves this simplex can be parameterized by a variable q constrained to an ellipsoid with curvature $D = \text{diag}(\dots, \langle v_i, Bv_i \rangle, \dots)$. This matches the analysis of EigenGame exactly, except that $D = I$ in that previous work. The implication is that each utility function as defined in equation (48) is also a cosine, but with its angular axis deformed according to D . \square

As an example consider setting

$$A = \begin{bmatrix} 0.77759061 & 0.26842584 \\ 0.26842584 & 0.87788983 \end{bmatrix} \quad B = \begin{bmatrix} 0.2325605 & 0.06042127 \\ 0.06042127 & 0.03241424 \end{bmatrix} \quad (24)$$

and observe the utilities in Figure 1.

Our proposed utilities tie nicely back to previous work (Gemp et al. (2022), Appx. J.2) via their gradients and our derived update directions.

Lemma 5 (Γ -EigenGame Gradient). *The gradient of player i 's utility with respect to \hat{v}_i is*

$$2 \times \left[\frac{(\hat{v}_i^\top B \hat{v}_i) A \hat{v}_i - (\hat{v}_i^\top A \hat{v}_i) B \hat{v}_i}{\langle \hat{v}_i, B \hat{v}_i \rangle^2} - \sum_{j < i} \frac{\hat{\lambda}_j}{\langle \hat{v}_j, B \hat{v}_j \rangle} (\hat{v}_i^\top B \hat{v}_j) \frac{[\langle \hat{v}_i, B \hat{v}_i \rangle B \hat{v}_j - \langle \hat{v}_i, B \hat{v}_j \rangle B \hat{v}_i]}{\langle \hat{v}_i, B \hat{v}_i \rangle^2} \right]. \quad (25)$$

Proof. Recall player i 's utility function:

$$u_i(\hat{v}_i | \hat{v}_{j < i}) = \underbrace{\hat{\lambda}_i}_{\text{reward}} - \sum_{j < i} \underbrace{\hat{\lambda}_j \langle \hat{y}_i, B \hat{y}_j \rangle^2}_{\text{penalty}} \quad \text{where } \hat{y}_i = \frac{\hat{v}_i}{\|\hat{v}_i\|_B}, \quad (26)$$

$$\hat{\lambda}_i = \frac{\langle \hat{v}_i, A \hat{v}_i \rangle}{\langle \hat{v}_i, B \hat{v}_i \rangle}, \text{ and } \|z\|_B = \sqrt{\langle z, Bz \rangle}.$$

We will address the gradient of each term in the chain rule in sequence. First consider $\hat{\lambda}_i$:

$$\nabla_{\hat{v}_i} \hat{\lambda}_i = \nabla_{\hat{v}_i} \left\{ \frac{\langle \hat{v}_i, A \hat{v}_i \rangle}{\langle \hat{v}_i, B \hat{v}_i \rangle} \right\} = \nabla_{\hat{v}_i} \left\{ \langle \hat{v}_i, A \hat{v}_i \rangle \langle \hat{v}_i, B \hat{v}_i \rangle^{-1} \right\} \quad (27)$$

$$= \frac{2(\hat{v}_i^\top B \hat{v}_i) A \hat{v}_i - 2(\hat{v}_i^\top A \hat{v}_i) B \hat{v}_i}{\langle \hat{v}_i, B \hat{v}_i \rangle^2}. \quad (28)$$

The next term that depends on \hat{v}_i is $\langle \hat{y}_i, B \hat{y}_j \rangle^2$ through \hat{y}_i :

$$\nabla_{\hat{v}_i} \langle \hat{y}_i, B \hat{y}_j \rangle^2 = \nabla_{\hat{v}_i} \left\{ \langle \hat{v}_i, B \hat{y}_j \rangle^2 \langle \hat{v}_i, B \hat{v}_i \rangle^{-1} \right\} \quad (29)$$

$$= 2 \langle \hat{v}_i, B \hat{y}_j \rangle B \hat{y}_j \langle \hat{v}_i, B \hat{v}_i \rangle^{-1} - \langle \hat{v}_i, B \hat{y}_j \rangle^2 \langle \hat{v}_i, B \hat{v}_i \rangle^{-2} (2B \hat{v}_i) \quad (30)$$

$$= \frac{2 \langle \hat{v}_i, B \hat{y}_j \rangle (\langle \hat{v}_i, B \hat{v}_i \rangle B \hat{y}_j - \langle \hat{v}_i, B \hat{y}_j \rangle B \hat{v}_i)}{\langle \hat{v}_i, B \hat{v}_i \rangle^2} \quad (31)$$

$$= \frac{2 \langle \hat{v}_i, B \hat{v}_j \rangle (\langle \hat{v}_i, B \hat{v}_i \rangle B \hat{v}_j - \langle \hat{v}_i, B \hat{v}_j \rangle B \hat{v}_i)}{\langle \hat{v}_i, B \hat{v}_j \rangle \langle \hat{v}_i, B \hat{v}_i \rangle^2} \quad (32)$$

where we have replaced all \hat{y}_j terms with $\frac{\hat{v}_j}{\langle \hat{v}_j, B \hat{v}_j \rangle^{1/2}}$ terms and consolidated the denominators.

Combining these intermediate results, we find

$$\nabla_{\hat{v}_i} u_i = 2 \left[\frac{(\hat{v}_i^\top B \hat{v}_i) A \hat{v}_i - (\hat{v}_i^\top A \hat{v}_i) B \hat{v}_i}{\langle \hat{v}_i, B \hat{v}_i \rangle^2} - \sum_{j < i} \frac{\hat{\lambda}_j}{\langle \hat{v}_j, B \hat{v}_j \rangle} (\hat{v}_i^\top B \hat{v}_j) \frac{[\langle \hat{v}_i, B \hat{v}_i \rangle B \hat{v}_j - \langle \hat{v}_i, B \hat{v}_j \rangle B \hat{v}_i]}{\langle \hat{v}_i, B \hat{v}_i \rangle^2} \right]. \quad (33)$$

□

Proposition 3 (Equivalence to EigenGame Unloaded). *The generalized EigenGame pseudogradient in equation (12) is equivalent to the Riemannian gradient in (Gemp et al., 2021) when $B = I$.*

Proof. In order to compute the Riemannian update direction, we project player i 's direction onto the tangent space of the unit-sphere by left-multiplying with $(I - \hat{v}_i \hat{v}_i^\top)$. Starting with equation (12),

we find

$$\tilde{\nabla}_i = \overbrace{(\hat{v}_i^\top B \hat{v}_i) A \hat{v}_i - (\hat{v}_i^\top A \hat{v}_i) B \hat{v}_i}^{\text{reward}} - \sum_{j < i} \overbrace{(\hat{v}_i^\top A \hat{v}_j) [\langle \hat{v}_i, B \hat{v}_i \rangle B \hat{v}_j - \langle \hat{v}_i, B \hat{v}_j \rangle B \hat{v}_i]}^{\text{penalty}} \quad (34)$$

$$= A \hat{v}_i - (\hat{v}_i^\top A \hat{v}_i) \hat{v}_i - \sum_{j < i} (\hat{v}_i^\top A \hat{v}_j) [\hat{v}_j - \langle \hat{v}_i, \hat{v}_j \rangle \hat{v}_i] \quad (35)$$

$$= (I - \hat{v}_i \hat{v}_i^\top) [A \hat{v}_i - \sum_{j < i} (\hat{v}_i^\top A \hat{v}_j) \hat{v}_j] = (I - \hat{v}_i \hat{v}_i^\top) \tilde{\nabla}_i^{\mu-EG}. \quad (36)$$

□

Proposition 4 (Γ -EigenGame Utilities as Deflated Rayleigh Quotients). *The generalized EigenGame utilities defined in equation (48) can also be derived from the perspective of maximizing the Rayleigh quotients of a deflated matrix assuming exact parents.*

Proof. Deflating a matrix means to modify the matrix such that the spectrum corresponding to a certain subspace of the matrix is zero. For example, in the case of the SGEP, the matrix A can be deflated to produce a matrix $\tilde{A} = (I - B \frac{v_j v_j^\top}{\|v_j\|_B^2}) A$ such that any vector in the span of eigenvector v_j achieves zero eigenvalue:

$$\tilde{A}(w_j v_j) = w_j (I - B \frac{v_j v_j^\top}{\|v_j\|_B^2}) A v_j \quad (37)$$

$$= w_j A v_j - w_j B v_j \frac{v_j^\top A v_j}{\|v_j\|_B^2} \quad (38)$$

$$= w_j \lambda_j B v_j - w_j \lambda_j B v_j \frac{v_j^\top B v_j}{\|v_j\|_B^2} \text{ apply rule } A v_j = \lambda_j B v_j \quad (39)$$

$$= w_j \lambda_j B v_j (1 - \frac{v_j^\top B v_j}{\|v_j\|_B^2}) \quad (40)$$

$$= 0 \quad (41)$$

where $\|v_j\|_B^2 = v_j^\top B v_j$ and w_j is an arbitrary scalar.

This is useful because it allows us to construct a top- k solver by induction: repeatedly deflate a matrix to ignore the top- $(j < i)$ eigenvectors and then deploy a top-1 solver on the deflated matrix to find the i th eigenvector. To that end, we can construct the following deflation matrix:

$$\tilde{A}_i = (I - \sum_{j < i} B \frac{v_j v_j^\top}{\|v_j\|_B^2}) A. \quad (42)$$

Note that this definition assumes the parents eigenvectors are exact. If they are approximate, this may not act as a deflation in the precise sense. For example, consider defining \tilde{A} with approximate \hat{v}_j instead of exact v_j . Now let $\hat{v}_j = v_1$ for all j . If one repeats the analysis above for a vector in the span of v_1 , they would find that equation (40) becomes $w_1 \lambda_1 B v_1 (1 - (i-1) \frac{v_1^\top B v_1}{\|v_1\|_B^2}) = w_1 \lambda_1 B v_1 (2-i)$, i.e., it results in an eigenvalue of $(2-i)\lambda_1$. This is why the effect of this matrix is more accurately described via penalties. We will clarify this connection next.

With the above preliminaries taken care of, we will now show how to derive our utilities via a deflation perspective. Initially, we will assume exact parents, $\hat{v}_{j<i} = v_{j<i}$.

$$u_i(\hat{v}_i | v_{j<i}) = \frac{\langle \hat{v}_i, \tilde{A}_i \hat{v}_i \rangle}{\langle \hat{v}_i, B \hat{v}_i \rangle} \quad (43)$$

$$= \frac{\langle \hat{v}_i, (I - \sum_{j<i} B \frac{v_j v_j^\top}{\|v_j\|_B^2}) A \hat{v}_i \rangle}{\langle \hat{v}_i, B \hat{v}_i \rangle} \quad (44)$$

$$= \frac{\langle \hat{v}_i, A \hat{v}_i \rangle}{\langle \hat{v}_i, B \hat{v}_i \rangle} - \sum_{j<i} \frac{\langle \hat{v}_i, B v_j v_j^\top A \hat{v}_i \rangle}{\|v_j\|_B^2 \langle \hat{v}_i, B \hat{v}_i \rangle} \text{ expand sum} \quad (45)$$

$$= \frac{\langle \hat{v}_i, A \hat{v}_i \rangle}{\langle \hat{v}_i, B \hat{v}_i \rangle} - \sum_{j<i} \frac{\langle \hat{v}_i, B v_j \rangle \langle \hat{v}_i, A v_j \rangle}{\langle v_j, B v_j \rangle \langle \hat{v}_i, B \hat{v}_i \rangle} \text{ split \& transpose inner product} \quad (46)$$

$$= \frac{\langle \hat{v}_i, A \hat{v}_i \rangle}{\langle \hat{v}_i, B \hat{v}_i \rangle} - \sum_{j<i} \frac{\lambda_j \langle \hat{v}_i, B v_j \rangle^2}{\langle v_j, B v_j \rangle \langle \hat{v}_i, B \hat{v}_i \rangle} \text{ apply rule } A v_j = \lambda_j B v_j \quad (47)$$

$$= \underbrace{\hat{\lambda}_i}_{\text{reward}} - \sum_{j<i} \underbrace{\lambda_j \langle \hat{y}_i, B y_j \rangle^2}_{\text{penalty}} \quad \text{where } \hat{y}_i = \frac{\hat{v}_i}{\|\hat{v}_i\|_B}, \quad (48)$$

$$\hat{\lambda}_i = \frac{\langle \hat{v}_i, A \hat{v}_i \rangle}{\langle \hat{v}_i, B \hat{v}_i \rangle}, \text{ and } \|z\|_B = \sqrt{\langle z, B z \rangle}.$$

If we then relax our assumption and allow v_j to be approximate ($v_j \rightarrow \hat{v}_j$) we recover our utilities in equation (48). \square

C SMOOTH AND UNBIASED

In order to prove asymptotic convergence of γ -EigenGame in the deterministic setting, we establish the following lemmas.

Lemma 6. *The update $\tilde{\nabla}_i$ in equation (7) is smooth.*

Proof. The reward terms are polynomial in \hat{v}_i and therefore smooth (analytic). The numerators of the penalty terms are also polynomial in \hat{v}_i and \hat{v}_j , however, the denominator includes a scalar $\langle \hat{v}_j, B \hat{v}_j \rangle$. Given $B \succ 0$, this term is guaranteed to be greater than the minimum eigenvalue of B (which is positive), thereby ensuring the penalty terms are non-singular. So these terms are also smooth. \square

Instead of proving the following lemmas directly for Algorithm 1 (the deterministic variant), we prove them for Algorithm 2, which subsumes Algorithm 1 ($\rho = 0, \gamma_t = 1, b = n, M = 1$).

The following two lemmas are proven in the single proof below. Note Lemma 7 is essentially a restatement of Lemma 2 from the main body.

Lemma 7. *The unique stable fixed point (up to sign of \hat{v}_j) of Algorithm 2 run with exact expectations (e.g., $n' = n$ where n is the full dataset size) is $\hat{v}_j = v_j$ for all $j \in \{1, \dots, k\}$, i.e., the top- k generalized eigenvectors.*

Lemma 8. *Algorithm 2's updates are asymptotically unbiased.*

Proof. The proof is constructed sequentially by proving each update process has a unique stable fixed point conditioned on the previous updates' fixed points defined by the hierarchy imposed on the players. We explain how we are able to address constructing unbiased estimates of each update as well, thereby supporting a stochastic, asymptotic convergence proof.

The proof begins by considering the updates of the first player on \hat{v}_1 . Player 1 is unique in that it pays no penalties for aligning with other players. Its update consists of the reward terms only, which comprises an unbiased estimate assuming independent, unbiased estimates for A and B (i.e., these are constructed with independent minibatches). Player 1's update simply performs Riemannian

gradient ascent on its utility function. Proposition 1 proves that every maximum of this function is a global maximum (in addition, it contains no saddle points). Therefore, the only stable fixed point for \hat{v}_1 is v_1 .

Next, we consider player 1’s update to $[B\hat{v}]_1$. Given we just showed \hat{v}_1 ’s stable fixed point is v_1 , and this update is simply a running average, its unique stable fixed point is Bv_1 .

We now consider player 2’s update, which includes penalty terms. Plugging $[B\hat{v}]_1$ ’s unique stable fixed point into these penalty terms, and again assuming independent, unbiased estimates for A and B , allows us to construct an unbiased estimate of the penalty terms. Similarly to player 1’s analysis, player 2’s update performs Riemannian gradient ascent on a utility function with a unique stable fixed point, $\hat{v}_2 = v_2$.

The proof then proceeds repeating the same arguments, alternating between proving the unique stable fixed point of each $[B\hat{v}]_j = Bv_j$ and $\hat{v}_j = v_j$. \square

D ERROR PROPAGATION

An error propagation analysis is necessary to rule out the scenario where an arbitrary (unbounded) level of precision is required by the parents to ensure any progress towards the true solution can be made by the children. In other words, we show that as the parents near their true solutions, the children may near theirs as well.

As before in Appx. C, we will perform this analysis for the stochastic version of the algorithm (Algorithm 2), but note that this subsumes the analysis for the deterministic version (where $[B\hat{v}]_j$ is replaced by the exact Bv_j with zero error).

Player 1’s update of \hat{v}_1 is unbiased without any assumptions on the state of any of the other player vectors $\hat{v}_{j>1}$ or auxiliary variables $[B\hat{v}]_{j\geq 1}$. We would like to understand how transient error in \hat{v}_1 propagates through to these other variables. The updates of player 1’s children depend on $[B\hat{v}]_1$, so we analyze the effect on it first. Note that the error propagation analysis naturally repeats as we progress down the hierarchy of players, so we analyze how error in \hat{v}_i propagates through to $[B\hat{v}]_i$ and then onto $\hat{v}_{j>i}$. Interestingly, step 2 of the following proof suggests the error in the \hat{v}_i must fall below $\frac{1}{\kappa}$ before any increase in accuracy of the parents helps to improve accuracy in the children. This result mirrors that of (Gemp et al., 2021) (see their Appendix F).

Theorem 3. *An $\mathcal{O}(\epsilon)$ angular error in the parent propagates to an $\mathcal{O}(\epsilon^{\frac{1}{2}})$ upper bound on the angular error of the child’s solution.*

Proof. The proof proceeds in three steps:

1. $\mathcal{O}(\epsilon)$ angular error of parent $v_i \implies \mathcal{O}(\epsilon)$ Euclidean error of parent v_i
2. $\mathcal{O}(\epsilon)$ Euclidean error of parent $v_i \implies \mathcal{O}(\epsilon)$ Euclidean error of norm of child $v_{j>i}$ ’s gradient
3. $\mathcal{O}(\epsilon)$ Euclidean error of norm child $v_{j>i}$ ’s gradient + instability of minima at $v_{k\neq j} \implies \mathcal{O}(\epsilon)$ angular error of child $v_{j>i}$ ’s solution assuming $B = I$.
4. $\mathcal{O}(\epsilon)$ angular error of child $v_{j>i}$ ’s solution assuming $B = I \implies \mathcal{O}(\epsilon^{\frac{1}{2}})$ angular error of child $v_{j>i}$ ’s solution for a general $B \succ 0$.

1. As in μ -EigenGame, an *angular error* of ϵ in the parent translates to ϵ *Euclidean error*. The proof is exactly the same as in (Gemp et al., 2021), repeated here for convenience. Angular error in the parent can be converted to Euclidean error by considering the chord length between the mis-specified parent and the true parent direction. The two vectors plus the chord form an isosceles triangle with the relation that chord length $l = 2 \sin(2\epsilon)$ is $\mathcal{O}(\epsilon)$ for $\epsilon \ll 1$.

2. Next, write the mis-specified parents as $\hat{v}_i = v_i + w_i$ where $\|w_i\|$ is $\mathcal{O}(\epsilon_i)$ as we just explained.

Now consider the fixed point of the auxiliary variable’s update: $[Bv]_i = B(v_i + w_i) = Bv_i + Bw_i$. Hence any mis-specification in the parent \hat{v}_i appears as a mis-specification of the auxiliary variable’s

fixed point by Bw_i , which is $\mathcal{O}(\lambda_{max}\epsilon)$ where λ_{max} is the maximum eigenvalue (spectral radius) of B . Assume the auxiliary variable is mis-specified by an additional error (q_i where $\|q_i\|$ is $\mathcal{O}(\epsilon'_i)$) representing failure to precisely reach the perturbed fixed point $B(v_i + w_i)$, i.e., $[B\hat{v}]_i = B(v_i + w_i) + q_i$.

The auxiliary variable impacts the update of $\hat{v}_{j>i}$ through \hat{y}_i and similarly $[B\hat{y}]_i$:

$$\hat{y}_i = \frac{\hat{v}_i}{\sqrt{[\langle \hat{v}_i, [B\hat{v}]_i \rangle]_\rho}} \quad (49)$$

$$= \frac{v_i + w_i}{\sqrt{[\langle \hat{v}_i, Bv_i \rangle + \langle \hat{v}_i, Bw_i \rangle + \langle \hat{v}_i, q_i \rangle]_\rho}} \quad (50)$$

$$= \frac{v_i + w_i}{\sqrt{[\langle v_i, Bv_i \rangle + 2\langle v_i, Bw_i \rangle + \langle w_i, Bw_i \rangle + \langle v_i, q_i \rangle + \langle w_i, q_i \rangle]_\rho}} \quad (51)$$

$$= cy_i + \frac{w_i}{\sqrt{[\langle v_i, Bv_i \rangle + 2\langle v_i, Bw_i \rangle + \langle w_i, Bw_i \rangle + \langle v_i, q_i \rangle + \langle w_i, q_i \rangle]_\rho}} \quad (52)$$

$$= cy_i + e_i \quad (53)$$

In order to bound this term, we make a few mild assumptions.

- Assume ρ is less than λ_{min} as stated earlier and, in particular, less than the lower bound.
- Assume ϵ'_i is $\mathcal{O}(\epsilon_i)$ to ease the exposition.
- Also, w.l.o.g., assume $\lambda_{max} > 1$; if not, we can simply scale the problem such that it is true.

Let $\kappa = \frac{\lambda_{max}}{\lambda_{min}}$ be the condition number of B , and note that the error term in the denominator is bounded by the spectrum of B :

$$[\langle \hat{v}_i, [B\hat{v}]_i \rangle]_\rho \leq \langle v_i, Bv_i \rangle + 2\lambda_{max}\epsilon_i + \lambda_{max}\epsilon_i^2 + \epsilon'_i + \epsilon_i\epsilon'_i \quad (54)$$

$$\stackrel{1 \leq \lambda_{max} \leq \kappa \langle v_i, Bv_i \rangle}{\leq} \langle v_i, Bv_i \rangle (1 + 2\kappa\epsilon_i + \kappa\epsilon_i^2 + \kappa\epsilon'_i + \kappa\epsilon_i\epsilon'_i) \quad (55)$$

$$\stackrel{\epsilon' \text{ is } \mathcal{O}(\epsilon)}{\leq} \langle v_i, Bv_i \rangle (1 + 3\kappa\epsilon_i + 2\kappa\epsilon_i^2) \quad (56)$$

and vice versa for the lower bound, which implies

$$(57)$$

$$[\langle \hat{v}_i, [B\hat{v}]_i \rangle]_\rho \in \langle v_i, [Bv]_i \rangle \left[(1 - 3\kappa\epsilon_i - 2\kappa\epsilon_i^2), (1 + 3\kappa\epsilon_i + 2\kappa\epsilon_i^2) \right]. \quad (58)$$

Then

$$c \in \left[\frac{1}{\sqrt{1 + 3\kappa\epsilon_i + 2\kappa\epsilon_i^2}}, \frac{1}{\sqrt{1 - 3\kappa\epsilon_i - 2\kappa\epsilon_i^2}} \right]. \quad (59)$$

Note that if $\epsilon_i \ll \frac{1}{\kappa}$, then c is $\mathcal{O}(1)$. Note this condition also implies e_i is $\mathcal{O}(\epsilon'_i)$. We will use these facts later.

Now we are prepared to consider the norm of the difference, d_j , between the Riemannian⁴ update to \hat{v}_j with exact parents and auxiliary variables versus the actual inexact Riemannian update. Let Δ_j^R be defined as in line 12 of Algorithm 2. Define $\hat{\Delta}_j^R$ to be the same except with \hat{y}_l and $[B\hat{y}]_l$ terms replaced by their true solution counterparts y_l and $[By]_l$. Note that Δ_j^R and $\hat{\Delta}_j^R$ already live in the tangent space of the unit-sphere at \hat{v}_j . Then the norm of the difference between the two update

⁴The Riemannian update projects the vanilla update onto the tangent space of the sphere.

directions is upper bounded as

$$\|d_j\| = \|\Delta_j^R - \bar{\Delta}_j^R\| \quad (60)$$

$$\leq \left\| \sum_{l < i} \left[(\hat{v}_j^\top A \hat{y}_l) [\langle \hat{v}_j, B \hat{v}_j \rangle [B \hat{y}]_l - \langle \hat{v}_j, [B \hat{y}]_l \rangle B \hat{v}_j] - \dots \right] \right\| \quad (61)$$

$$\leq \sum_{l < i} \left\| \left[(\hat{v}_j^\top A \hat{y}_l) [\langle \hat{v}_j, B \hat{v}_j \rangle [B \hat{y}]_l - \langle \hat{v}_j, [B \hat{y}]_l \rangle B \hat{v}_j] - \dots \right] \right\|. \quad (62)$$

Recall q_i is the error associated with suboptimality of $[B \hat{v}]_i$ and propogates to $[B \hat{y}]_i$ as defined on line 9 of Algorithm 2. Let

$$p_i = \frac{q_i}{\sqrt{[\langle v_i, B v_i \rangle + 2 \langle v_i, B w_i \rangle + \langle w_i, B w_i \rangle + \langle v_i, q_i \rangle + \langle w_i, q_i \rangle]_\rho}}. \quad (63)$$

By similar arguments used to bound e_i , $\|p_i\|$ is $\mathcal{O}(\epsilon_i')$ if $\epsilon_i \ll \frac{1}{\kappa}$.

Bounding the summand in equation (62), we find

$$\|(\hat{v}_j^\top A \hat{y}_l) [\langle \hat{v}_j, B \hat{v}_j \rangle [B \hat{y}]_l - \langle \hat{v}_j, [B \hat{y}]_l \rangle B \hat{v}_j] - (\hat{v}_j^\top A y_l) [\langle \hat{v}_j, B \hat{v}_j \rangle [B y]_l - \langle \hat{v}_j, [B y]_l \rangle B \hat{v}_j]\| \quad (64)$$

$$= \|(\hat{v}_j^\top A y_l + \hat{v}_j^\top A e_l) [\langle \hat{v}_j, B \hat{v}_j \rangle (c B y_l + B e_l + p_l) - \langle \hat{v}_j, (c B y_l + B e_l + p_l) \rangle B \hat{v}_j] - \dots\| \quad (65)$$

$$= \|(c^2 - 1)(\hat{v}_j^\top A y_l) [\langle \hat{v}_j, B \hat{v}_j \rangle B y_l - \langle \hat{v}_j, B y_l \rangle B \hat{v}_j] + \mathcal{O}(\epsilon)\|. \quad (66)$$

Recall equation (59) and note that

$$c^2 - 1 \in \left\{ \frac{-3\kappa\epsilon_i - 2\kappa\epsilon_i^2}{1 + 3\kappa\epsilon_i + 2\kappa\epsilon_i^2}, \frac{3\kappa\epsilon_i + 2\kappa\epsilon_i^2}{1 - 3\kappa\epsilon_i - 2\kappa\epsilon_i^2} \right\} \quad (67)$$

which has norm $|c^2 - 1| = \mathcal{O}(\kappa\epsilon_i)$. Therefore, taking into account the impact of the other A and B terms, $\|d_j\|$ is upper bounded by $\mathcal{O}(i\kappa\sigma(A)\lambda_{\max}^2\epsilon_i)$ where $\sigma(A)$ is the spectral radius of A .

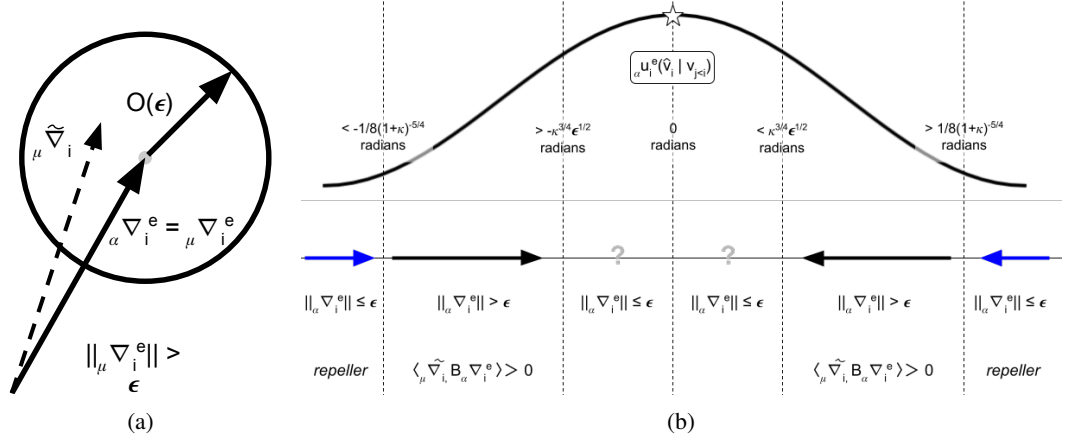


Figure 5: (a) Close in Euclidean distance can imply close in angular distance if the vectors are long enough (reprinted with permission from (Gemp et al., 2021)). (b) The stable region may consist of an $\mathcal{O}(\kappa^{3/4}\epsilon^{1/2})$ ball around the true optimum as $\epsilon \rightarrow 0$.

3. We can reuse the analysis of (Gemp et al., 2021) to understand how a change in the norm of the vector field relates to a change in the location of the fixed point. This is because the Riemannian update direction of our proposed method with exact parents and $B = I$ is equivalent to the Riemannian update direction in (Gemp et al., 2021) (simply left-multiply their equation (4) by $(I - \hat{v}_i \hat{v}_i^\top)$ to compute their Riemannian update). Therefore, as in this prior work, an error in the gradient norm translates to the same order of error in angular distance to the true fixed point (inflated by a finite scaling dependent on the spectrum of B —accounted for in Step 4 next).

Also, the region around any generalized eigenvector $v_{l \neq j}$ is unstable and this is because the Riemmanian Hessian at that point is positive (this implies instability because we are maximizing). We can reason that the Riemmanian Hessian is positive by appealing to the fact that the Riemmanian Hessian of our generalized EVP utilities is related to the Hessian of prior work by a warping defined by the positive definite matrix B (for a visual, see Figure 1; for math, see Lemmas 1 and 4).

In contrast to this prior work, the generalized eigenvectors are more generally, B -orthogonal (see Lemma 3). By Lemma 9, the angular distance between generalized eigenvectors is finite and depends on the condition number of B . Therefore, there exists a small enough ϵ such that an ϵ -ball around any *unstable* region and an ϵ -ball around the *stable* region no longer overlap.

4. Lastly, Lemma 10 proves that an $\epsilon_i < 1$ angular error assuming $B = I$ can be increased to at most $\kappa^{\frac{3}{4}} \epsilon_i^{\frac{1}{2}}$ if B is relaxed to be any symmetric positive definite matrix with condition number κ . \square

Lemma 9. *The angle between a pair of orthonormal vectors when instead measured under a general positive definite matrix C is lower bounded by $\frac{1}{8}(1 + \kappa)^{-\frac{5}{4}}$ where κ is the condition number of C , i.e., if $\langle v_i, v_j \rangle = 0$, then $|\theta| = \arccos\left(\frac{|\langle C^{\frac{1}{2}} v_i, C^{\frac{1}{2}} v_j \rangle|}{\|C^{\frac{1}{2}} v_i\| \|C^{\frac{1}{2}} v_j\|}\right) > \frac{1}{8}(1 + \kappa)^{-\frac{5}{4}}$ radians.*

Proof. The angle between two vectors is a function of their relation to each other in the two-dimensional plane defined by their pair. Therefore, without loss of generality, consider two vectors $u = \begin{bmatrix} 1 & 0 \end{bmatrix}$ and $v = \begin{bmatrix} 0 & 1 \end{bmatrix}$ and consider the effect of an arbitrary positive definite matrix \hat{C} on their angle. For ease of exposition, denote $\tau = \kappa^{\frac{1}{2}}$ the condition number of $C^{\frac{1}{2}}$.

Let $\hat{C}^{\frac{1}{2}} = \begin{bmatrix} a & c \\ c & b \end{bmatrix}$ be the unique positive definite square root of \hat{C} where a and b are positive and the determinant $ab - c^2 > \gamma > 0$. We aim to show that the magnitude of the angle between u and v under the generalized inner product $\langle \cdot, \cdot \rangle_C$ is lower bounded by a finite, positive quantity dependent on the properties of C .

Consider

$$\hat{C}^{\frac{1}{2}} u = \begin{bmatrix} a \\ c \end{bmatrix}, \quad \hat{C}^{\frac{1}{2}} v = \begin{bmatrix} c \\ b \end{bmatrix}, \quad (68)$$

$$\|\hat{C}^{\frac{1}{2}} u\| = \sqrt{a^2 + c^2}, \quad \|\hat{C}^{\frac{1}{2}} v\| = \sqrt{c^2 + b^2}, \quad (69)$$

$$\langle \hat{C}^{\frac{1}{2}} u, \hat{C}^{\frac{1}{2}} v \rangle = c(a + b). \quad (70)$$

Then

$$\frac{\langle \hat{C}^{\frac{1}{2}} u, \hat{C}^{\frac{1}{2}} v \rangle}{\|\hat{C}^{\frac{1}{2}} u\| \|\hat{C}^{\frac{1}{2}} v\|} = \frac{c(a + b)}{\sqrt{(a^2 + c^2)(c^2 + b^2)}} \quad (71)$$

$$\underbrace{\text{ratio is inc. in } c \text{ for } ab > c^2}_{<} \frac{\sqrt{ab - \gamma}(a + b)}{\sqrt{(a^2 + ab - \gamma)(ab + b^2 - \gamma)}} \quad (72)$$

$$\underbrace{\text{div. num. \& den. by } \frac{1}{a^2}}_{=}} \frac{\sqrt{\frac{b}{a} - \frac{\gamma}{a^2}}(1 + \frac{b}{a})}{\sqrt{(1 + \frac{b}{a} - \frac{\gamma}{a^2})(\frac{b}{a} + (\frac{b}{a})^2 - \frac{\gamma}{a^2})}} \quad (73)$$

$$\underbrace{\text{ratio is inc. in } \frac{b}{a}}_{\leq}} \frac{\sqrt{\tau - \frac{\gamma}{a^2}}(1 + \tau)}{\sqrt{(1 + \tau - \frac{\gamma}{a^2})(\tau + \tau^2 - \frac{\gamma}{a^2})}} \quad (74)$$

$$\underbrace{\text{ratio is inc. in } \tau - \frac{\gamma}{a^2}}_{<}} \frac{\sqrt{\tau - \frac{\gamma}{a^2}}(1 + \tau)}{\sqrt{(1 + \tau - \frac{\gamma}{a^2})(\tau + \tau^2 - \frac{\gamma}{a^2})}}. \quad (75)$$

Note that $\frac{b}{a}$ is a lower bound on the condition number of \hat{C} ; $\frac{b}{a}$ is equal to the condition number of $\hat{C}^{\frac{1}{2}}$ when $c = 0$ (assuming $b > a$, otherwise, $\frac{b}{a} < \frac{a}{b}$ clearly), and the condition number can only increase as c deviates from 0. Lastly, note that the condition number of $\hat{C}^{\frac{1}{2}}$ is upper bounded by τ , the condition number of $C^{\frac{1}{2}}$. Recall, by replacing $\frac{b}{a}$ with a larger number τ and $\frac{\gamma}{a^2}$ with a strictly smaller number $\frac{\gamma}{tr^2}$, $\frac{b}{a} - \frac{\gamma}{a^2}$ implies that $\tau > \frac{\gamma}{tr^2}$.

Now consider

$$\left(\frac{\langle C^{\frac{1}{2}}u, C^{\frac{1}{2}}v \rangle}{\|C^{\frac{1}{2}}u\| \|C^{\frac{1}{2}}v\|} \right)^2 < \frac{(\tau - \frac{\gamma}{tr^2})(1 + \tau)^2}{(1 + \tau - \frac{\gamma}{tr^2})(\tau + \tau^2 - \frac{\gamma}{tr^2})} \quad (76)$$

$$= \frac{(\tau - \frac{\gamma}{tr^2})(1 + \tau)^2}{(\tau - \frac{\gamma}{tr^2})(1 + \tau)^2 + (\frac{\gamma}{tr^2})^2} \quad (77)$$

$$= 1 - \frac{(\frac{\gamma}{tr^2})^2}{(\tau - \frac{\gamma}{tr^2})(1 + \tau)^2 + (\frac{\gamma}{tr^2})^2} \quad (78)$$

$$\leq 1 - \frac{(\frac{\gamma}{tr^2})^2}{(\tau)(1 + \tau)^2 + (1 + \tau)^2} \quad (79)$$

$$= 1 - \frac{(\frac{\gamma}{tr^2})^2}{(1 + \tau)^3}. \quad (80)$$

We can also simplify the fraction $\frac{\gamma}{tr^2}$. γ is a lower bound on the determinant, which is equal to the product of eigenvalues of $\hat{C}^{\frac{1}{2}}$. This is lower bounded by λ_{min}^2 for any two-dimensional subspace, therefore, $\lambda_{min}^2 < \gamma$. Furthermore, the trace of the matrix is equal to the sum of its eigenvalues. This is upper bounded by $2\lambda_{max}$ for any two-dimensional subspace, therefore $\frac{\gamma}{tr^2} > \frac{\lambda_{min}^2}{4\lambda_{max}^2} = \frac{1}{4\tau^2} > \frac{1}{4(\tau+1)^2}$.

Note that $|\theta| \geq |\sin(\theta)|$. Therefore,

$$|\theta| \geq |\sin(\theta)| = \sqrt{1 - \cos^2(\theta)} \quad (81)$$

$$> \sqrt{\frac{(\frac{\gamma}{tr^2})^2}{(1 + \tau)^3}} \quad (82)$$

$$> \frac{1}{2} \sqrt{(1 + \tau)^{-5}} \quad (83)$$

$$= \frac{1}{2} (1 + \tau)^{-\frac{5}{2}}. \quad (84)$$

Clearly this bound is loose as it implies θ is only greater than $2^{-\frac{7}{2}}$ for $C = I$ ($\tau = 1$) whereas we know in that case that $\theta = \frac{\pi}{2}$. However, this bound serves its purpose of establishing a finite impact of C on the orthogonality of the original two vectors, i.e., if u and v are orthogonal, their angle as measured under a generalized inner product by $C \succ 0$ cannot be 0.

Replacing τ with $\kappa^{\frac{1}{2}}$, we can further simplify the bound to

$$|\theta| > \frac{1}{2} (1 + \tau)^{-\frac{5}{2}} \quad (85)$$

$$\geq \frac{1}{8} (1 + \kappa)^{-\frac{5}{4}}. \quad (86)$$

□

Lemma 10. *The angle between a pair of nearly parallel vectors ($|\theta|$ is $\mathcal{O}(\epsilon)$ with $\epsilon \ll 1$) when instead measured under a general positive definite matrix C is upper bounded by $\mathcal{O}(\kappa^{\frac{3}{4}} \epsilon^{\frac{1}{2}})$.*

Proof. Let $C^{\frac{1}{2}} = \begin{bmatrix} a & c \\ c & b \end{bmatrix}$ be the unique positive definite square root of C where a and b are positive and the determinant $ab - c^2 > 0$. Consider a vector $u = \begin{bmatrix} 1 & 0 \end{bmatrix}$ and another vector

$v = \begin{bmatrix} \sqrt{1-\epsilon^2} & \epsilon \end{bmatrix}$ that is nearly parallel to u , i.e., $\epsilon \ll 1$ (implies $|\theta|$ is $\mathcal{O}(\epsilon)$). We aim to show that the angle between these two vectors under the generalized inner product $\langle \cdot, \cdot \rangle_C$ is upper bounded by a constant multiple of ϵ given a small enough ϵ .

Consider

$$C^{\frac{1}{2}}u = \begin{bmatrix} a \\ c \end{bmatrix}, \quad C^{\frac{1}{2}}v = \begin{bmatrix} a\sqrt{1-\epsilon^2} + c\epsilon \\ c\sqrt{1-\epsilon^2} + b\epsilon \end{bmatrix}, \quad (87)$$

$$\|C^{\frac{1}{2}}u\| = \sqrt{a^2 + c^2} \quad \|C^{\frac{1}{2}}v\| = \sqrt{a^2(1-\epsilon^2) + c^2\epsilon^2 + b^2\epsilon^2 + c^2(1-\epsilon^2)} \quad (88)$$

$$= a\sqrt{1 + (c/a)^2}, \quad = \sqrt{a^2 + c^2 + \epsilon^2(b^2 - a^2)} \quad (89)$$

$$= a\sqrt{1 + (c/a)^2 + \epsilon^2((b/a)^2 - 1)}, \quad (90)$$

and

$$\langle C^{\frac{1}{2}}u, C^{\frac{1}{2}}v \rangle = a^2\sqrt{1-\epsilon^2} + acc\epsilon + c^2\sqrt{1-\epsilon^2}b\epsilon \quad (91)$$

$$= (a^2 + c^2)\sqrt{1-\epsilon^2} + (a+b)c\epsilon \quad (92)$$

$$= a^2(1 + (c/a)^2)\sqrt{1-\epsilon^2} + a^2(1 + (b/a))(c/a)\epsilon \quad (93)$$

$$\stackrel{|\epsilon| < 1}{\geq} a(1 + (c/a)^2)(1 - \epsilon^2) + a^2(1 + (b/a))(c/a)\epsilon. \quad (94)$$

Then

$$\frac{\langle C^{\frac{1}{2}}u, C^{\frac{1}{2}}v \rangle}{\|C^{\frac{1}{2}}u\| \|C^{\frac{1}{2}}v\|} \geq \frac{(1 + (c/a)^2)(1 - \epsilon^2) + (1 + (b/a))(c/a)\epsilon}{(1 + (c/a)^2)\sqrt{1 + \epsilon^2 \frac{(b/a)^2 - 1}{(c/a)^2 + 1}}} \quad (95)$$

$$= \frac{1}{\sqrt{1 + \epsilon^2 \frac{(b/a)^2 - 1}{(c/a)^2 + 1}}} + \frac{(1 + (b/a))(c/a)\epsilon - (1 + (c/a)^2)\epsilon^2}{(1 + (c/a)^2)\sqrt{1 + \epsilon^2 \frac{(b/a)^2 - 1}{(c/a)^2 + 1}}} \quad (96)$$

$$\stackrel{b/a \leq \kappa}{\geq} \frac{1}{\sqrt{1 + \epsilon^2 \kappa^2}} + \frac{(1 + (b/a))(c/a)\epsilon - (1 + (c/a)^2)\epsilon^2}{(1 + (c/a)^2)\sqrt{1 + \epsilon^2 \frac{(b/a)^2 - 1}{(c/a)^2 + 1}}} \quad (97)$$

$$= 1 - \left(1 - \frac{1}{\sqrt{1 + \epsilon^2 \kappa^2}}\right) + \frac{(1 + (b/a))(c/a)\epsilon - (1 + (c/a)^2)\epsilon^2}{(1 + (c/a)^2)\sqrt{1 + \epsilon^2 \frac{(b/a)^2 - 1}{(c/a)^2 + 1}}} \quad (98)$$

$$\stackrel{c \geq -\sqrt{ab}}{\geq} 1 - \left(1 - \frac{1}{\sqrt{1 + \epsilon^2 \kappa^2}}\right) - \frac{(1 + (b/a))\sqrt{(b/a)}|\epsilon| - (1 + (c/a)^2)\epsilon^2}{(1 + (c/a)^2)\sqrt{1 + \epsilon^2 \frac{(b/a)^2 - 1}{(c/a)^2 + 1}}} \quad (99)$$

$$= 1 - \left(1 - \frac{1}{\sqrt{1 + \epsilon^2 \kappa^2}}\right) - \frac{(1 + (b/a))\sqrt{(b/a)}|\epsilon|}{(1 + (c/a)^2)\sqrt{1 + \epsilon^2 \frac{(b/a)^2 - 1}{(c/a)^2 + 1}}} - \frac{\epsilon^2}{\sqrt{1 + \epsilon^2 \frac{(b/a)^2 - 1}{(c/a)^2 + 1}}} \quad (100)$$

$$\stackrel{b/a \leq \kappa}{\geq} 1 - \left(1 - \frac{1}{\sqrt{1 + \epsilon^2 \kappa^2}}\right) - \frac{(1 + \kappa)\sqrt{\kappa}|\epsilon|}{\sqrt{1 - \epsilon^2}} - \frac{\epsilon^2}{\sqrt{1 - \epsilon^2}} \quad (101)$$

$$\stackrel{1 - \frac{1}{\sqrt{1+\kappa^2}} \leq \frac{\kappa}{2}, \epsilon^2 < \frac{1}{\kappa^2}}{\geq} 1 - \frac{\epsilon^2}{2} \kappa^2 - \frac{(1 + \kappa)\sqrt{\kappa}|\epsilon|}{\sqrt{1 - \epsilon^2}} - \frac{\epsilon^2}{\sqrt{1 - \epsilon^2}} \quad (102)$$

$$\stackrel{\epsilon < \frac{1}{2}}{\geq} 1 - 2(1 + \kappa)\sqrt{\kappa}|\epsilon| - \frac{\epsilon^2}{2}(\kappa^2 - 1) - 2\epsilon^2. \quad (103)$$

Note that $\cos(\theta) \leq 1 - \frac{1}{8}\theta^2$ for $|\theta| \leq \pi$. Then

$$|\theta| \leq 2\sqrt{2}\sqrt{1 - \cos(\theta)} \leq 2\sqrt{2}\sqrt{2(1 + \kappa)\sqrt{\kappa}|\epsilon| + \left(\frac{\kappa^2}{2} + 2\right)\epsilon^2} \quad (104)$$

$$\leq 4\sqrt{(1 + \kappa)\sqrt{\kappa}|\epsilon| + \left(\frac{\kappa^2}{4} + 1\right)\epsilon^2}. \quad (105)$$

Therefore, for $\epsilon < \min(\frac{1}{\kappa}, \frac{1}{2})$, $\arccos\left(\frac{|\langle C^{\frac{1}{2}}u, C^{\frac{1}{2}}v \rangle|}{\|C^{\frac{1}{2}}u\| \|C^{\frac{1}{2}}v\|}\right)$ is upper bounded by $\mathcal{O}(\epsilon^{\frac{1}{2}}\kappa^{\frac{3}{4}})$.

□

E ASYMPTOTIC CONVERGENCE

We carryout a proof of convergence of Algorithm 1 in the deterministic setting and a partial proof of Algorithm 2 with further discussion.

E.1 ASYMPTOTIC CONVERGENCE OF DETERMINISTIC UPDATE

We now give the convergence proof of Algorithm 1 using the theoretical results established above.

Theorem 2 (Deterministic / Full-batch Global Convergence). *Given a symmetric matrix A and symmetric positive definite matrix B where the top- k eigengaps of $B^{-1}A$ are positive along with a square-summable, not summable step size sequence η_t (e.g., $1/t$), Algorithm 1 converges to the top- k eigenvectors asymptotically ($\lim_{T \rightarrow \infty}$) with probability 1.*

Proof. Assume none of the \hat{v}_i are initialized to an angle exactly at the minimum of their utility. This is a set of vectors with Lebesgue measure 0, therefore, the assumption holds w.p.1.

Denote the “update field” $H(\hat{V})$ to match the work of (Shah, 2019). $H(\hat{V})$ is simply the concatenation of all players’ Riemannian update rules, i.e., all players updating in parallel using their Riemannian updates:

$$H(\hat{V}) = [\Delta_1, \dots, \Delta_k] : \mathbb{R}^{kd} \rightarrow \mathbb{R}^{kd} \quad (106)$$

where Δ_i is defined in equation (7) and \hat{V} represents the set of all \hat{v}_i .

A Riemannian gradient ascent step (with retractions) is then given by the following update step:

$$\hat{V}(t+1) \leftarrow \hat{V}(t) + \eta_t H(\hat{V}(t)) \quad (107)$$

$$\hat{v}_i(t+1) \leftarrow \hat{v}_i(t+1) / \|\hat{v}_i(t+1)\| \quad \forall i. \quad (108)$$

By Lemma 7, v_1 is the unique fixed point of \hat{v}_1 ’s update. And by Theorem 3, convergence of v_1 to within $\mathcal{O}(\epsilon)$ of its fixed point contributes to a mis-specification of children $\hat{v}_{j>1}$ ’s fixed point by $\mathcal{O}(\sqrt{\epsilon})$. Critically, this mis-specification is shrinking in ϵ so that as \hat{v}_1 nears its fixed point, so may its children. This chain of reasoning applies for all \hat{v}_i .

The result is then obtained by applying Theorem 7 of Shah (2019) with the following information: **A0**) the unit-sphere is a compact manifold with an injectivity radius of π which implies the injectivity radius of the manifold of the game (the product space of k unit-spheres) is also finite, **A1**) the update field is smooth (analytic) by Lemma 6, **A2**) we assume a square-summable, not summable step size, **A3**) we assume the full-batch (noiseless) setting so the update “noise” clearly constitutes a bounded martingale difference sequence, and **A4**) the iterates remain bounded because they are constrained to the unit-sphere.

Formally, for any $T > 0$,

$$\lim_{s \rightarrow \infty} \sup_{t \in [s, s+T]} d(\hat{V}(t), \hat{V}^s(t)) \rightarrow a.s., \quad (109)$$

where $d(\cdot, \cdot)$ is the Riemannian distance on the (product space of) sphere and $\hat{V}^s(t)$ denotes the continuous time trajectory of $H(\hat{V})$ starting from $\hat{V}(s)$. □

E.2 ASYMPTOTIC CONVERGENCE OF STOCHASTIC UPDATE

There are two primary issues with extending the asymptotic convergence guarantee in Theorem 2 to Algorithm 2. The first is that the joint parameter space includes $\hat{v}_i \in \mathcal{S}^{d-1}$ and $[B\hat{v}]_i \in \mathbb{R}^d$. The unit-sphere, \mathcal{S}^{d-1} , is a compact Riemannian manifold. While \mathbb{R}^d is a Riemannian manifold, it is not compact. This violates assumptions **A0** and **A4** above. The second issue is that the vector field $H(\hat{V}; [B\hat{V}])$ is not smooth due to the clipped denominator terms of y_j (see line 8 of Algorithm 2). We can easily fix this issue with a change of variables, defining $\langle \hat{v}_i, B\hat{v}_i \rangle$ in log-space. This results in Algorithm 3.

Specifically, define $[\langle v, Bv \rangle]_j = e^{\log(\rho) + (\log(\nu) - \log(\rho)) \text{sigmoid}(z_j)}$ where z_j is a newly introduced auxiliary variable. The relevant gradient with respect z_j is $\nabla_{z_j} = -(\langle v_j, Bv_j \rangle - [\langle v, Bv \rangle]_j) \cdot [\langle v, Bv \rangle]_j \cdot (\log \nu - \log \rho) \cdot \text{sigmoid}(z_j) \cdot (1 - \text{sigmoid}(z_j))$.

Regarding the still unresolved first issue, we could constraint $[B\hat{v}]_i$ to a ball with radius $\lambda_{\max}(B)$ centered at the origin, which is a convex set. Note that while a ball in \mathbb{R}^d is compact, it is not a Riemannian manifold anymore. A few works have developed theory for the setting that mixes convex and Riemannian optimization (Liu et al., 2017; Goyal & Shetty, 2019). Intuitively, we do not expect issues arising in our setting from the mixture of feasible sets, however, progress towards theoretic results takes time. We conjecture that Algorithm 3 is provably asymptotically convergent, although Algorithm 2 defined with clipping is a bit more practical.

Algorithm 3 Smooth Stochastic γ -EigenGame

-
- 1: Given: paired data streams $X_t \in \mathbb{R}^{b \times d_x}$ and $Y_t \in \mathbb{R}^{b \times d_y}$, number of parallel machines M per player (minibatch size per machine $b' = \frac{b}{M}$), step size sequence η_t , scalar ρ lower bounding $\lambda_{\min}(B)$, scalar, ν upper bounding $\lambda_{\max}(B)$, and number of iterations T .
 - 2: $\hat{v}_i \sim \mathcal{S}^{d-1}$, i.e., $\hat{v}_i \sim \mathcal{N}(\mathbf{0}_d, \mathbf{I}_d)$; $\hat{v}_i \leftarrow \hat{v}_i / \|\hat{v}_i\|$ for all i
 - 3: $[B\hat{v}]_i \in \mathbb{R}^d \leftarrow \hat{v}_i$ for all i
 - 4: $z_i^0 \in \mathbb{R} \leftarrow 0$ for all i
 - 5: **for** $t = 1 : T$ **do**
 - 6: **parfor** $i = 1 : k$ **do**
 - 7: **parfor** $m = 1 : M$ **do**
 - 8: Construct A_{tm} and B_{tm}
 - 9: $[\langle v, Bv \rangle]_j = e^{\log(\rho) + (\log(\nu) - \log(\rho)) \sigma(z_j)}$
 - 10: $\hat{y}_j = \frac{\hat{v}_j}{\sqrt{[\langle v, Bv \rangle]_j}}$
 - 11: $[B\hat{y}]_j = \frac{[B\hat{v}]_j}{\sqrt{[\langle v, Bv \rangle]_j}}$
 - 12: rewards $\leftarrow (\hat{v}_i^\top B_{tm} \hat{v}_i) A_{tm} \hat{v}_i - (\hat{v}_i^\top A_{tm} \hat{v}_i) B_{tm} \hat{v}_i$
 - 13: penalties $\leftarrow \sum_{j < i} (\hat{v}_i^\top A \hat{y}_j) [\langle \hat{v}_i, B_{tm} \hat{v}_i \rangle [B\hat{y}]_j - \langle \hat{v}_i, [B\hat{y}]_j \rangle B_{tm} \hat{v}_i]$
 - 14: $\tilde{\nabla}_{im} \leftarrow \text{rewards} - \text{penalties}$
 - 15: $\nabla_{im}^{Bv} = (B_{tm} \hat{v}_i - [B\hat{v}]_i)$
 - 16: $\nabla_{im}^z = (\langle v_i, [Bv]_i \rangle - [\langle v, Bv \rangle]_i) \cdot [\langle v, Bv \rangle]_i \cdot (\log \nu - \log \rho) \cdot \sigma(z_i) \cdot (1 - \sigma(z_i))$
 - 17: **end parfor**
 - 18: $\tilde{\nabla}_i \leftarrow \frac{1}{M} \sum_m [\tilde{\nabla}_{im}]$
 - 19: $\hat{v}'_i \leftarrow \hat{v}_i + \eta_t \tilde{\nabla}_i$
 - 20: $\hat{v}_i \leftarrow \frac{\hat{v}'_i}{\|\hat{v}'_i\|}$
 - 21: $\nabla_i^{Bv} \leftarrow \frac{1}{M} \sum_m [\nabla_{im}^{Bv}]$
 - 22: $[B\hat{v}]_i \leftarrow [B\hat{v}]_i + \gamma_t \nabla_i^{Bv}$
 - 23: $\nabla_i^z \leftarrow \frac{1}{M} \sum_m [\nabla_{im}^z]$
 - 24: $z_i \leftarrow z_i + \gamma_t \nabla_i^z$
 - 25: **end parfor**
 - 26: **end for**
 - 27: **return** all \hat{v}_i
-

F ALTERNATIVE PARALLELIZED IMPLEMENTATION

As mentioned in Section 5, we plan to open source our implementation, specifically the implementation used to conduct the neural CCA experiments described in Section 5. The specific parallelization we used was different than that implied by Algorithm 2. Instead, we parallelized the estimation of the matrix-vector products $A\hat{v}_i$ and $B\hat{v}_i$ for all i and then aggregated this information across machines. Figure 6 provides a diagram illustrating how data and algorithmic operations are distributed.

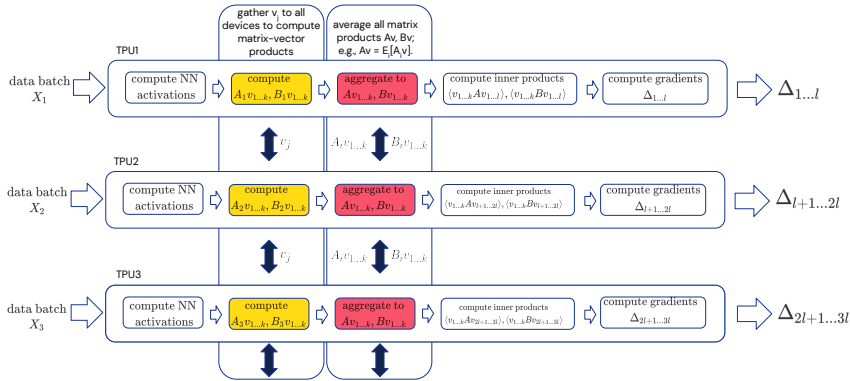


Figure 6: Parallelization of γ -EigenGame implementation for neural CCA experiments in Section 5.

G ADDITIONAL EXPERIMENTS

G.1 REGULARIZATION EFFECTS OF STOCHASTIC APPROXIMATION

In pursuit of understanding the regularization benefits of our stochastic approximation approach with a fixed step size, we explore various ways of regularizing the matrices A and B prior to calling `scipy.linalg.eigh(A, B)` to see if we can achieve a similar solution. Figure 7 explores various parameter settings, but none adequately recover the original signals.

We parameterize our regularizations as follows. Let $C = \mathbb{E}_t[x_t x_t^\top]$. Then

$$A = \mathbb{E}_t[\langle x_t, x_t \rangle x_t x_t^\top] - \text{tr}(C + \epsilon)(C + \epsilon) - 2(C + \epsilon)^2 \quad B = C + \epsilon'. \quad (110)$$

G.2 PARALLEL VS SEQUENTIAL LEARNING

The parallel approach provides a few advantages over the sequential approach. 1) Intuitively, the parallel approach is similar to the sequential approach but with “warm starting”. Child eigenvectors are allowed to learn while their parents are learning, which puts them in a good position to reach their correct directions once their parents have learned. In contrast, a sequential approach would randomly initialize the child once the parents have converged, leaving the child to traverse a longer geodesic to reach its true destination. 2) How do you know when the parents are done learning? You would need to measure convergence of the eigenvectors and this is difficult in the stochastic setting. You could use a running mean of the Riemannian gradient norm or of the difference in successive Rayleigh quotients, but this is approximate. This is an interesting challenge for future research.

In Figure 8, we assume we know the true eigenvalues and use this information to decide when to deflate. In this experiment, the first two eigenvalues are approximated well enough, but this level of accuracy is not high enough to allow learning the third eigenvector accurately. This supports our argument where knowing when to stop learning and deflate is a difficult problem because the accuracy of parents affects the learning of children in ways that depend on the spectrum (which is unknown in any practical setting).

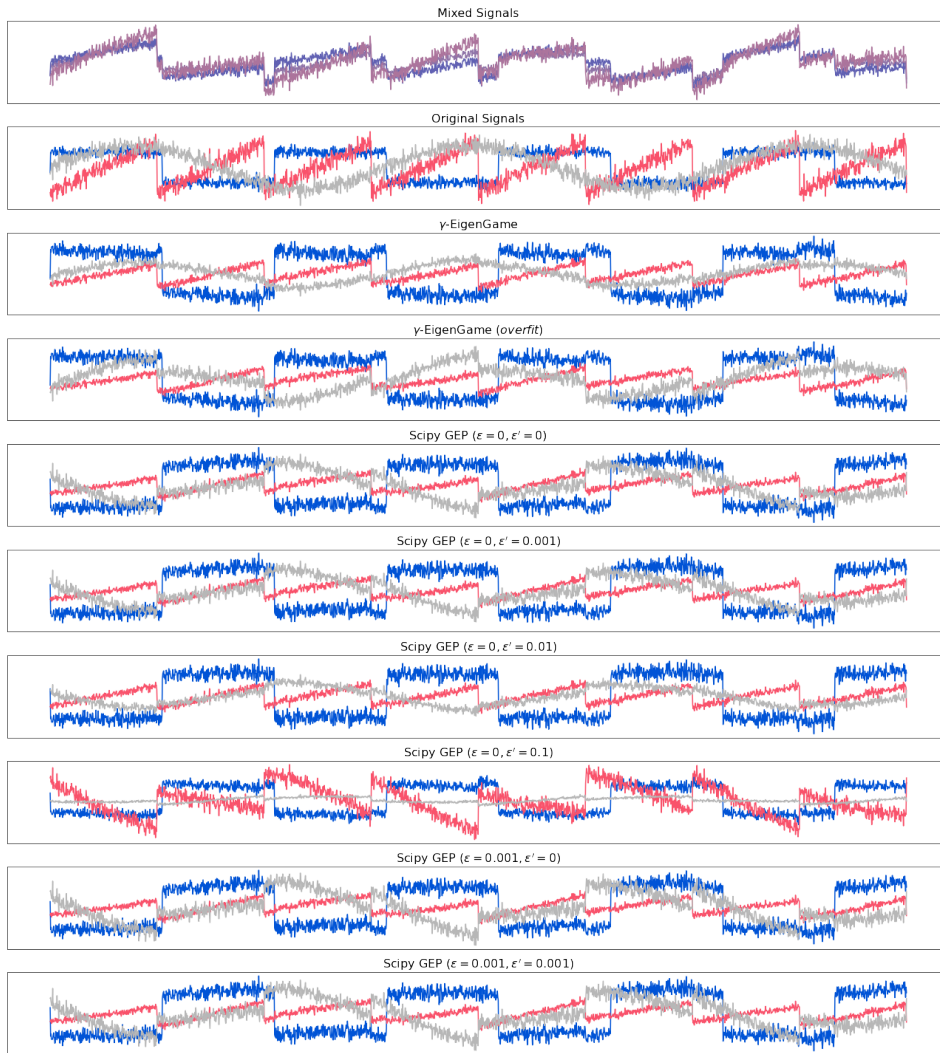


Figure 7: Figure 2 repeated with additional regularized versions of `scipy.linalg.eigh`.

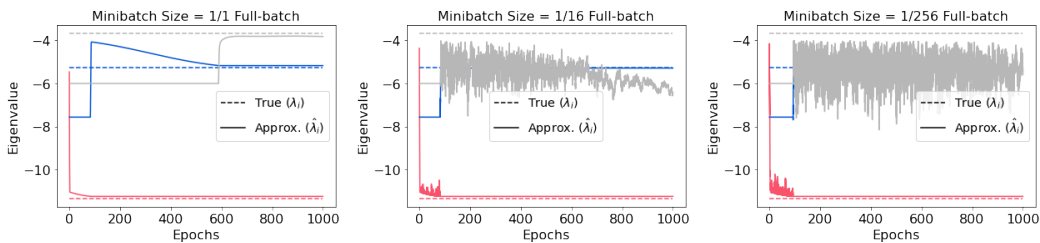


Figure 8: In contrast to the parallel learning approach we propose in Algorithm 2, here, we explore a sequential, deflation-inspired approach where each eigenvector completes learning only once its Rayleigh quotient (eigenvalue) is within 0.1 of the true value (we chose this value of 0.1 because full batch EigenGame (Figure 2 (left)) reaches at least 0.1 accuracy for all 3 eigenvalues by the end of training). Once this eigenvector has completed learning, the next eigenvector then begins learning. This sequential approach fails to learn the third eigenvalue to within the 0.1 threshold in both minibatch settings.

H HYPERPARAMETERS AND EXPERIMENT DETAILS

H.1 ICA

Details of the unmixing experiment we run can be found on the scikit-learn website: [./auto_examples/decomposition/plot_ica_blind_source_separation.html](https://auto-examples.decomposition/plot_ica_blind_source_separation.html) (Pedregosa et al., 2011). We solve for top-3 SGEP formulation of ICA using $n = 2000$ samples taken from the time series data. Minimal hyperparameter tuning was performed. Learning rates were searched over orders of magnitude (e.g., 0.01, 0.1, 1.0, ...).

H.1.1 COMPARISON

The parameters used for Algorithm 2 (γ -EigenGame) in Figure 2 are listed in Table 1. Those for overfitting γ -EigenGame to the data are listed in Table 2.

batch size b	$\frac{n}{4}$
M	1
# of iterations (T)	$10^3 \cdot \frac{n}{b}$
η_t	$10^{-2} \cdot \frac{b}{n}$
β_t	$1 \cdot \frac{b}{n}$

Table 1: Algorithm 2 hyperparameters for γ -EigenGame in Figure 2.

batch size b	n
M	1
# of iterations (T)	10^5
η_t	10^{-3}
β_t	1

Table 2: Algorithm 2 hyperparameters for γ -EigenGame (*overfit*) in Figure 2.

H.1.2 UNBIASED

Each of the plots in Figure 3 uses a different minibatch size b ; the hyperparameters used for Algorithm 2 are listed in Table 3 as a function of b .

M	1
# of iterations (T)	$10^3 \cdot \frac{n}{b}$
η_t	$10^{-2} \cdot \frac{b}{n}$
β_t	$1 \cdot \frac{b}{n}$

Table 3: Algorithm 2 hyperparameters for Figure 3.

H.2 CCA

Details of both CCA experiments can be found below.

H.2.1 COMPARISON

Hyperparameters for the algorithm proposed in (Meng et al., 2021) are the same as in their paper. Their code is available on github at `.../zihangm/riemannian-streaming-cca`. We ran experiments 10 times to produce the means and standard deviation shading in Figure 2. We run PCA first on the data to remove the subspaces in X and Y with zero variance. We then solve the top-4 SGEP formulation of CCA. Hyperparameters were tuned manually, searching over orders of magnitude (e.g., 0.01, 0.1, 1.0 and in some cases 0.05, 0.5, 5.0). We set $\rho = 10^{-10}$.

Shared parameters	
b	100
M	1
T	$\frac{n}{b}$
MNIST	
η_t	0.1
β_t	1.0
Mediamill	
η_t	50
β_t	5
CIFAR-10	
η_t	0.1
β_t	0.1

Table 4: Algorithm 2 hyperparameters for Figure 2.

H.2.2 NEURAL NETWORK ANALYSIS

We trained two CNNs for the $d > 10^3$ and $d > 10^5$ CCA (top-1024 SGEP) experiments in Figure 4. Details of both architectures are listed in Table 5.

We used the hyperparameters listed in Table 6 for running γ -EigenGame.

Adam($b1 = 0.9, b2 = 0.999, \epsilon = 10^{-8}$) was used for learning \hat{v}_i . We pair Adam with a learning rate schedule that consists of separate warmup and harmonic decay phases. We have a warmup period for the eigenvectors while the auxiliary variables and mean estimates are learned. During this period, the learning rate increases linearly until it reaches the base learning rate after the period ends (iteration t_c). This is followed by a decaying learning rate ($\propto \frac{1}{t+\Delta t}$) which reaches the final learning rate at iteration T .

For the purpose of generating the plots, we estimated Rayleigh quotients with a larger batch size than that used to estimate the eigenvectors themselves; specifically, we used 2048 for evaluation vs 256 for training.

Both experiments were 100% input bound, meaning the bottleneck in speed was computing neural network activations and passing them in minibatches to our algorithm. Therefore, our current runtimes are not indicative of the complexity of our proposed update rule. Alternatively, one could precompute all activations and save them to disk, however, this is memory intensive and we chose not to do this. For completeness, the $d > 10^3$ dimensional experiment ran at 4.7 ms per step on average, and the 10^5 experiment at 30.2 ms per step.

$d = 2048 > 10^3$ - Figure 4 (left)

Activations Harvested	Last convolutional layer and dense layer
Conv Layer Output Channels	[64, 32]
Conv Strides	[2, 1]
Dense Layer Sizes	[512]
Total Activations	$d_x = d_y = 1024$

$d = 116736 > 10^5$ - Figure 4 (right)

Activations Harvested	All convolutional layers and dense layer
Conv Layer Output Channels	[128, 256, 512]
Conv Strides	[1, 1, 1]
Dense Layer Sizes	[1024]
Total Activations	$d_x = d_y = 58368$

Table 5: CNN architecture parameters for CIFAR-10 Neural CCA experiment.

Algorithm Parameters

b	2048 (256 per device)
M	8 (2×2 TPU = 4 chips, 2 devices/chip)
T	10^7
η_t	$t_c = 10^5, \eta_0 = 10^{-4}, \eta_T = 10^{-6}$
β_t	10^{-3}
ϵ	10^{-4}
ρ	10^{-6}

Table 6: Algorithm 2 (with parallelism modifications from Section F) hyperparameters for Figure 4.

We do not have a breakdown of the runtime that separates CIFAR-10 data loading from neural network evaluation (computing activations) from EigenGame update from other processes. However, we can share that overall, the $d > 10^3$ dimensional experiment ran at 4.7 ms per step on average, and the 10^5 experiment at 30.2 ms per step.

I RUNTIME COMPLEXITY

Algorithm 2 states under line 1 "Given" that it expects "number of parallel machines M per player". There are k players, established in Section 2. This means Algorithm 2 expects $p = kM$ processors. This can also be inferred by noticing the two parallel for-loops (parfor) on lines 5 and 6 of Algorithm 2. The paragraph on "Computational Complexity and Parallelization" then goes on to consider the case where "each player (model) parallelizes over $M = b$ machines" where b is the batch size. Again, referring back to Algorithm 2, it is written "minibatch size per machine $b' = \frac{b}{M}$ ", therefore, $b' = 1$. We can now consider the computational cost of each line of Algorithm 2, which is dominated by the matrix-vector products on lines 8-11. Recall that A_{tm} and B_{tm} are both formed as outer products, e.g., $B_{tm} = X_{tm}^\top X_{tm}$ in ICA with $X_{tm} \in \mathbb{R}^{b' \times d}$. Given that we are considering the case where $b' = 1$, B_{tm} can be rewritten as $x_{tm}x_{tm}^\top$ where $x_{tm} \in \mathbb{R}^d$ to make it clear that the $1 \times d$ matrices are vectors. Therefore, all matrix-vector products (and inner products) on lines 8-11

cost $\mathcal{O}(d)$. There is 1 on line 8, 1 on line 9, 4 on line 10 (rewards), and $4k$ on line 11 (penalties) making for a total cost of $\mathcal{O}(dk)$.